Supporting Information for: Multiplex and In Vivo Optical Imaging of Discrete Luminescent Lanthanide Complexes Enabled by In Situ Cherenkov Radiation Mediated Energy Transfer

Kirsten E. Martin, Alexia G. Cosby and Eszter Boros [a, *]

[a)] Department of Chemistry, Stony Brook University, 100 Nicolls road, Stony Brook, NY 11794, USA

Table of Contents

1. Experimental Procedures

1.1 General Methods

All starting materials were purchased from commercial sources and used without further purification. **NMR spectra** (^{1}H, ^{13}C) were collected on a 700 MHz Advance III Bruker, 500 MHz, or 400 MHz Bruker instrument at 25 °C and processed using TopSpin 4.0.7. Chemical shifts are reported as parts per million (ppm). **Low resolution electrospray ionization (ESI) mass spectrometry** was carried out at the Stony Brook University Institute for Chemical Biology and Drug Discovery (ICB&DD) Mass Spectrometry Facility with an Agilent LC/MSD. **High resolution ESI mass spectrometry** was carried out at the Stony Brook University Center for Advanced Study of Drug Action (CASDA) with a Bruker Impact II UHR QTOF MS system. **UV-VIS** spectra were collected with the NanoDrop One^{C} instrument. Spectra were recorded from 200 to 900 nm in a quartz cuvette with 1 cm path length. **Luminescence measurements** were carried out on a Hitachi F-7100 FL spectrophotometer. Wavelength scans were collected by exciting at the appropriate wavelength (283 nm for Eu(III) and 282 for Tb(III)) for antenna-mediated excitation and minimization of scattering interference. Emission spectra were collected from 300 to 800 nm, with 1.0 nm excitation and 5.0 nm emission slit widths, 1200 s scan time, 0.05 s response time, and PMT voltage = 400 V. Quantum yield measurements for europium were carried out using $Ru(bipy)_3$ as standard (λ_{ex} = 450 nm). Terbium quantum yield measurements used $[Tb(DO3Apic)]^-$ (QY= 47%)[1] as a standard. **Lifetime measurements** were executed using the following settings: scan time 20 ms; chopping speed of 40 Hz; excitation wavelength of 255 nm, (with the exception of $[Eu(DO2Aphen)]^+$ which was excited at 285 nm) and emission wavelength of 555 nm; 0-second delay; excitation and emission slit widths of 10 nm each; 0.5 second response. Complexes were dissolved in H_2O or D_2O and samples were resuspended and lyophilized in D_2O repeatedly prior to measurement. A quartz cuvette with a 1 cm pathlength was used. **ICP-OES**

was carried out using an Agilent 5110 inductively coupled plasma optical emission spectrometer. A 10-point standard curve or a 6-point standard curve with respect to europium or terbium was used and fits were found to be at least R^2 of 0.999. Concentrations were back calculated to determine the stock sample concentration. Concentrations of each lanthanide complex were diluted and 200 μL aliquots of dilutions were prepared in 1X DPBS buffer to which 10 μL of $Na^{18}F$ (10 or 20 μCi) was added to produce a final volume of 210 μL. **IVIS** Lumina Series III from Caliper LifeSciences small animal imager was used for all imaging experiments. Scans were collected over 5 minutes with blocked excitation and either open emission filter (500 nm to 875 nm, with an average band width of 20 nm) or selected emission filters for multiplexed imaging (40 nm bandpass emission filters centered at 570 nm for window 1, and 620 nm for window 2). Images were analyzed with Living Image software (version 4.3.1). Regions of interest were determined in triplicate with the ROI tool for each concentration. Radiance values for each complex are subtracted from the Cherenkov-only sample ($Na^{18}F$ in 1X DPBS buffer). Error bars indicate average error in ROI sampling, n=3.

All **HPLC purification and analytical methods** were conducted using a binary solvent system in which solvent A was water + 0.1% TFA and solvent B was MeCN + 0.1% TFA. Preparative HPLC was carried out on a Phenomenex Luna C18 column (250 mm × 21.2 mm, 100 Å, AXIA packed) at a flow rate of 15 mL/min using a Shimadzu HPLC-20AR equipped with a binary gradient pump, UV-vis detector, and manual injector. UV absorption was recorded at 254 nm. Method A: Gradient: 0–1 min: 5% B; 1–14 min: 5–50% B; 14–23 min: 50–95% B; 23–26 min: 95% B; 26–27 min: 95–5% B; 27–30 min: 5% B. **Flash chromatography** was carried out using a Combi Flash Rf+ on a RediSep column (100 g HP C18 gold, CV: 87.7 mL, flow rate: 60 mL/min). Method B: Gradient: 1-2 min 10% B; 2-3 min: 10–20% B; 3–19 min: 20–25% B; 19 min: 25-

100% B; 19-23 min: 100% B; 23 min: 100-10% B; 23-25 min: 10% B. **Analytical HPLC** was carried out on a Phenomenex Luna 5 μm C18 column (150 mm × 3 mm, 100 Å, AXIA packed) at a flow rate of 0.8 mL/min using either a Shimadzu HPLC-20AR equipped with a binary gradient pump, UV-vis detector, autoinjector, and Laura radiodetector or Agilent 1260 Infinity II HPLC. UV absorption was recorded at 254 nm. Method C: (Shimadzu system) Gradient: 0–2 min: 5% B; 2–14 min: 5–95% B; 14–16 min: 95% B; 16–16.5 min: 95–5% B; 16.5–20 min 5% B. Method D: 0–16 min: 5–95% B

Synthesis and Characterization

Macrocyclic starting materials tri-tert-butyl 1,4,7,10-tetraazacyclododecane-1,4,7-triacetate (DO3A^{t}Bu)[2] and tert-Butyl [7-(tert-butoxycarbonylmethyl)-1,4,7,10-tetraaza-1-cyclododecyl]acetate (DO2A^{t}Bu)[3] were prepared according to literature procedures. (R)-2-(3-((R)-4-(5-aminopentylamino)-4-oxo-1-tert-butoxycarbonylbutyl)ureido)glutarate[4] and (13*S*,17*S*)-1-(4,10-bis(carboxymethyl)-7-((6-carboxypyridin-2-yl)methyl)-1,4,7,10-tetraazacyclododecan-1-yl)-2,10,15-trioxo-3,9,14,16-tetraazanonadecane-13,17,19-tricarboxylic acid ((DO2Apic)-DUPA)[5] and [Tb(DO3Apic)]$^{-}$.[1] were synthesized according to a previously reported procedures.

1.2 Synthesis of [Eu(DO3Aphen)]

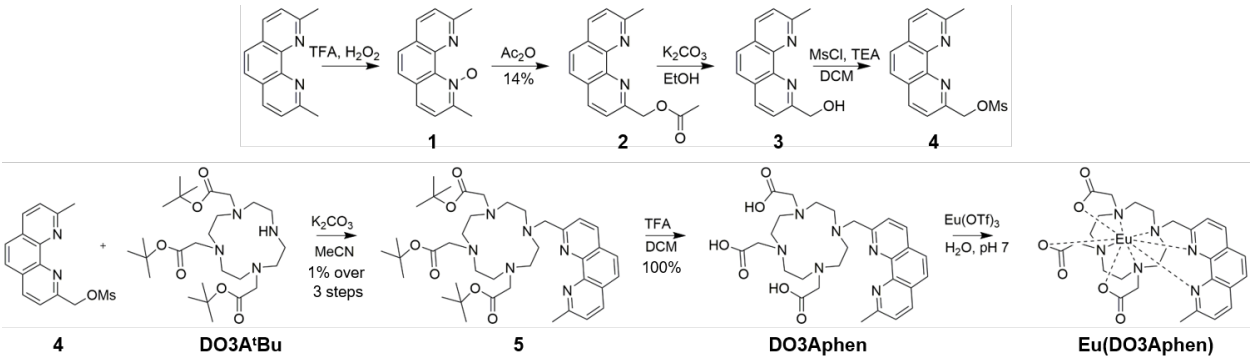

Scheme S1. Synthetic scheme for [Eu(DO3Aphen)]

2-(acetoxymethyl)-9-methyl-l,10-phenanthroline (2)

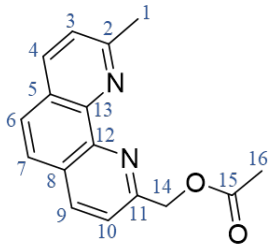

Acetic anhydride (0.8 mL) was added to a solution of 2,9-dimethyl-l,10-phenanthroline N-oxide **(1)** (124.8 mg, 0.557 mmol)[6] in DCM. The DCM was subsequently removed in vacuo and the solution was refluxed for 1 hour. The mixture was concentrated in vacuo and then dissolved in $CHCl_3$ and washed with saturated aqueous Na_2CO_3 (75 mL). The organic layer was dried over Na_2SO_4 and the solvent was removed under reduced pressure to give a dark brown oil . The crude product was purified using flash chromatography (Method B) with pure product eluting at 22% B. Fractions containing product were pooled and concentrated to give **2** as a yellow oil (21.5 mg, 14% yield). ^{1}H NMR (CD_3OD, 700 MHz): δ 9.13 (d, 1H, H^9), 8.68 (d, 1H, H^4), 8.26 (d, 1H, H^3), 8.20 (q, 2H, $H^{6,7}$), 8.05 (d, 1H, H^{10}), 5.61 (s, 2H, H^{14}), 3.19 (s, 3H, H^1), 2.23 (s, 3H, H^{16}). ESI-MS calcd. for $C_{16}H_{14}N_2O_2$: 266.11. Found: 267.1 $[M+H]^+$.

tert-Butyl{4-[(6-methyl-4,5-diaza-3-phenanthryl)methyl]-7,10-bis(tert-butoxycarbonylmethyl)-1,4,7,10-tetraaza-1-cyclododecyl}acetate (5)

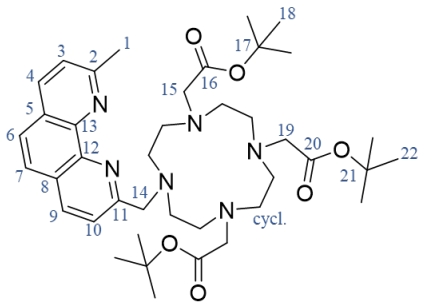

A suspension of **2** (315.0 mg, 1.184 mmol) and K_2CO_3 (273.0 mg, 1.978 mmol) in absolute EtOH (15 mL) was stirred at room temperature for 6 hours. The reaction mixture was filtered, and the filtrate was concentrated in vacuo. The residue was triturated with DCM to afford **3**, which was then used immediately without purification. The residue was solubilized in dry DCM (8 mL) and triethylamine (239 µL, 1.71 mmol) was added. Methanesulfonyl chloride (110 µL, 1.42 mmol) was then added and the mixture was allowed to stir at room temperature for 4 hours. The mixture was washed with brine and solvent was removed in vacuo. The product **(4)** was used immediately for alkylation. The product was combined with DO3A^{tBu} [2](44.0 mg, 0.085 mmol) and K_2CO_3 (117.0 mg, 0.845 mmol) in dry MeCN (10 mL). The mixture was refluxed for 18 hours. The K_2CO_3 was filtered, and the solvent concentrated in vacuo. The resulting oil was purified with reverse phase preparative HPLC (Method A) with the product eluting at 15.7 min. The fractions containing product were combined and the solvent was removed in vacuo to afford **5** as a white solid (9.2 mg, 1% yield over three steps.) ^{1}H NMR (CD_3OD, 700MHz): δ 8.63 (br d, 2H, $H^{9,4}$), 8.11 (m, 3H, $H^{3,6,7}$), 7.98 (s, 1H, H^{10}), 4.98 (s, 2H, H^{14}), 4.59-3.35 (m, 16H, $H^{15,19,\ cycl}$), 3.27-2.93 (m, 6H, H^{cycl}), 3.07 (s, 3H, H^1), 1.56 (s, 9H, H^{22}), 1.29 (s, 18H, H^{18}). $^{13}C\{^1H\}$ NMR (CD_3OD, 175 MHz): δ 172.5 (C^{16}), 166.9 (C^{20}), 160.2 (C^2), 152.9 (C^{11}), 143.5 (C^4), 141.3 (C^9), 139.3 ($C^{12,13}$), 130.5 (C^8), 129.3 (C^5), 128.3 ($C^{6,7}$), 127.8 (C^3) 126.9 (C^{10}), 86.0 (C^{21}), 83.3 (C^{17}), 59.6 (C^{cycl}), 56.0 (C^{cycl}), 55.5 ($C^{15,19}$), 52.8 (C^{cycl}), 50.5 (C^{cycl}), 49.9 (C^{14}), 28.5 (C^{22}), 28.4 (C^{18}), 24.0 (C^1). ESI- MS calcd. for $C_{40}H_{60}N_6O_6$: 720.46. Found: 721. 5 $[M+H]^+$.

{4,10-Bis(carboxymethyl)-7-[(6-methyl-4,5-diaza-3-phenanthryl)methyl]-1,4,7,10-tetraaza-1-cyclododecyl}acetic acid (DO3Aphen)

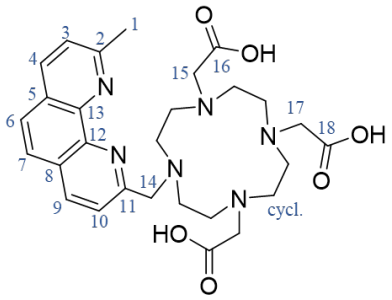

5 (13.3 mg, 0.018 mmol) was dissolved in a solution of 1:2 DCM:TFA (3 mL) and stirred at room temperature overnight. The solvent was removed in vacuo, and the product was re-dissolved in H_2O. The solution was then lyophilized to yield **DO3Aphen** as a white solid (18.5 mg, 100% yield). Additional mass can be accounted for by residual TFA salts. ^{1}H NMR (CD_3OD, 700MHz): δ 9.03 (d, 1H, H^{9}), 8.73 (s, 1H, H^{4}), 8.24 (q, 2H, $H^{6,7}$), 8.07 (d, 2H, $H^{3,10}$), 4.96 (s, 2H, H^{14}), 4.16 (s, 2H, H^{17}), 3.73-3.35 (m, 12H, $H^{15,cycl}$), 3.16 (s, 3H, H^{1}), 3.29-2.98 (m, 8H, H^{cycl}). ^{13}C{^{1}H} NMR (CD_3OD, 175 MHz): δ 174.9 ($C^{16,18}$), 160.7 (C^{2}), 145.5 (C^{11}), 140.8 (C^{4}), 140.5 (C^{9}), 138.8 ($C^{12,13}$), 130.9 (C^{8}), 129.4 (C^{5}), 128.4 ($C^{6,7}$), 127.8 (C^{3}), 127.5 (C^{10}), 60.3 ($C^{15,17}$), 55.5 (C^{cycl}), 54.8 (C^{cycl}), 52.3(C^{cycl}), 50.6 (C^{cycl}), 49.8 (C^{14}), 22.1 (C^{1}). HRMS calcd. for $C_{28}H_{36}N_6O_6$: 552.2969. Found: 553.2771 $[M+H]^+$. HPLC: t_R= 5.6 min (Method C).

1.3 Synthesis of $[Eu(DO2Aphen)]^+$

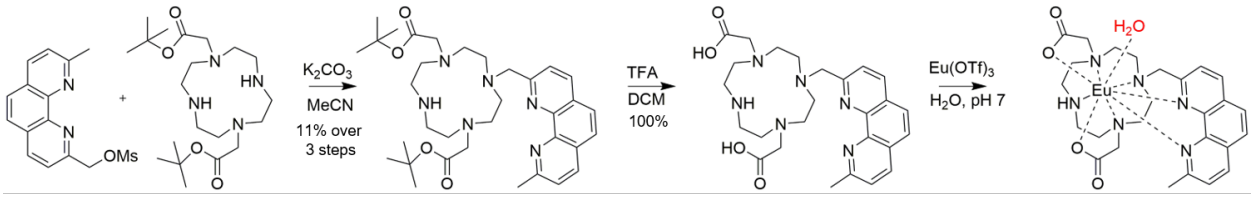

Scheme 2. Synthetic scheme for $[Eu(DO2Aphen)]^+$

tert-Butyl {4-[(6-methyl-4,5-diaza-3-phenanthryl)methyl]-7-(tert-butoxycarbonylmethyl)-1,4,7,10-tetraaza-1-cyclododecyl}acetate (6)

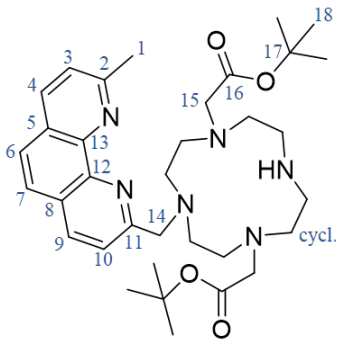

A suspension of **2** (18.1 mg, 0.068 mmol) and K_2CO_3 (15.7 mg, 0.114 mmol) in absolute EtOH (5 mL) was stirred at room temperature for 6 hours. The reaction mixture was filtered, and the filtrate was concentrated in vacuo. The residue was triturated with DCM to afford **3**, which was then used immediately without purification. Triethylamine (11.5 µL, 0.082 mmol) was added to a solution of the product in dry DCM (8 mL). Methanesulfonyl chloride (10.5 µL, 0.136 mmol) was then added and the mixture was allowed to stir at room temperature for 4 hours. The mixture was washed with brine and then the solvent was removed in vacuo. The product, **4**, was used immediately for alkylation. The product was combined with DO2A^{tBu} (27.2 mg, 0.068 mmol) and K_2CO_3 (46.8 mg, 0.339 mmol) in dry MeCN (10 mL). The mixture was stirred at room temperature for 18 hours. The mixture was filtered, and the solvent concentrated in vacuo. The resulting oil was purified with reverse phase preparative HPLC (Method A) with the product eluting at 14.5 min. The fractions containing product were combined and the solvent was removed in vacuo to afford **6** as a white solid (4.6 mg, 11% yield over 3 steps). ^{1}H NMR (CD_3OD, 700MHz): δ 8.82 (d, 1H, H^9), 8.67 (d, 1H, H^4), 8.16 (q, 2H, $H^{6,7}$), 8.06 (d, 1H, H^3), 8.01 (d, 1H, H^{10}), 4.98 (s, 2H, H^{14}), 3.72-3.48 (m, 5H, $H^{cycl, 15}$), 3.30-2.82 (m, 15H, $H^{cycl, 15}$), 3.10 (s, 3H, H^1), 1.33 (s, 18H, H^{18}). $^{13}C\{^1H\}$ NMR (CD_3OD, 175 MHz): δ 173.0 (C^{16}), 160.4 ($C^{2,11}$), 139.8 ($C^{12,13}$), 130.9 ($C^{4,9}$), 129.5 ($C^{5,8}$), 128.5 ($C^{6,7}$), 128.3 (C^3), 127.1 (C^{10}), 83.7 (C^{17}), 59.4 (C^{15}), 56.0 (C^{cycl}), 53.4 (C^{14}), 50.9 (C^{cycl}), 50.0 (C^{cycl}), 43.9 (C^{cycl}). 28.5 (C^{18}), 23.7 (C^1). ESI- MS calcd. for $C_{34}H_{50}N_6O_4$: 606.39. Found: 607.4 $[M+H]^+$.

{7-(Carboxymethyl)-4-[(6-methyl-4,5-diaza-3-phenanthryl)methyl]-1,4,7,10-tetraaza-1-cyclododecyl}acetic acid (DO2Aphen)

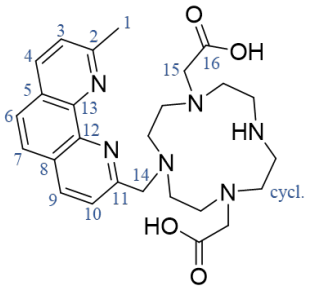

6 (22.0 mg, 0.036 mmol) was dissolved in a solution of 1:2 DCM:TFA (3 mL) and stirred at room temperature overnight. The solvent was removed in vacuo, and the product was re-dissolved in H_2O. The solution was then lyophilized to yield **DO2Aphen** as a white solid (19.3 mg, 100% yield). Additional mass can be accounted for by residual TFA salts. ^{1}H NMR (CD_3OD, 500MHz): δ 9.05 (d, 1H, H^9), 8.78 (d, 1H, H^4), 8.26 (q, 2H, $H^{6,7}$), 8.16 (d, 1H, H^3), 8.05 (d, 1H, H^{10}), 5.06 (s, 2H, H^{14}), 3.77-3.10 (m, 20H, $H^{15,\ cycl}$), 3.08 (s, 3H, H^1). $^{13}C\{^1H\}$ NMR (CD_3OD, 125 MHz): δ 176.0 (C^{16}), 160.4 (C^2), 153.1 (C^{11}), 145.7 (C^4), 140.7 (C^9), 131.2 ($C^{12,13}$), 129.7 (C^8), 129.5 (C^5), 128.5 ($C^{6,7}$), 127.8 (C^3), 127.5 (C^{10}), 59.5 (C^{15}), 55.9 (C^{cycl}), 53.8 (C^{cycl}), 50.9 (C^{cycl}), 50.5 (C^{cycl}), 44.3 (C^{14}), 21.5 (C^1). HRMS calcd. for $C_{26}H_{34}N_6O_4$: 494.2642. Found: 495.2712 $[M+H]^+$. HPLC: t_R= 5.7 min (Method C).

1.4 Synthesis of [Eu(DO2Aphen-DUPA)]$^+$

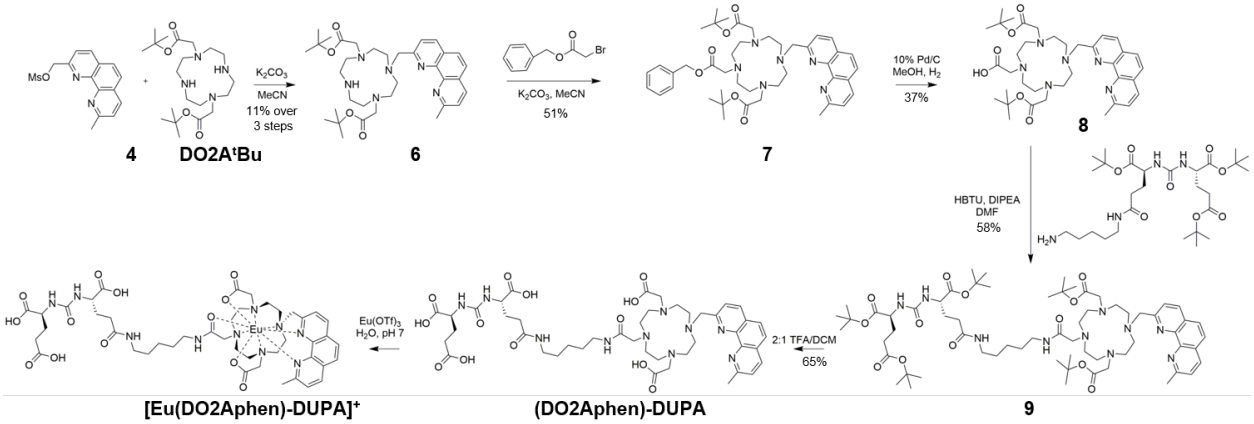

Scheme S3. Synthesis scheme of [Eu(DO2Aphen)-DUPA]$^+$

Benzyl{7-[(6-methyl-4,5-diaza-3-phenanthryl)methyl]-4,10-bis(tert-butoxycarbonylmethyl)-1,4,7,10-tetraaza-1-cyclododecyl}acetate (7)

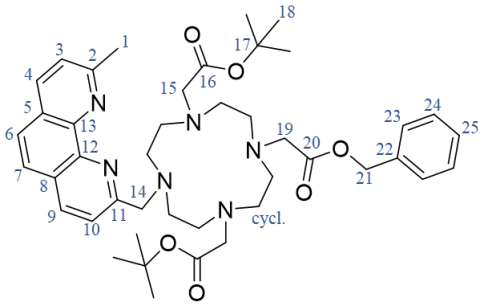

Benzyl bromoacetate (2.9 µL, 0.018 mmol), **6** (7.4 mg, 0.012 mmol), and K_2CO_3 (16.9 mg, 0.122 mmol) were combined in dry MeCN (5 mL) and refluxed overnight. K_2CO_3 was filtered, and the filtrate was concentrated. The resulting residue was purified using reverse phase preparative HPLC (Method A) with pure product eluting at 16.6 min. Fractions containing product were pooled and solvent was removed in vacuo to afford pure **7** (4.7 mg, 51% yield). ^{1}H NMR (CD_3OD, 700MHz): δ 9.06 (br s, 1H, H^9), 8.24 (m, 5H, $H^{3,4,6,7,10}$), 7.44 (m, 5H, $H^{23,24,25}$), 5.36 (s, 2H, H^{14}), 5.19, 4.16 (s, 2H, H^{21}), 4.03-3.33 (m, 16H, $H^{cycl,15,19}$), 3.30-3.02 (m, 16H, $H^{cycl,15,19}$), 3.19 (s, 3H, H^1), 1.40 (s, 18H, H^{18}). $^{13}C\{^1H\}$ NMR (CD_3OD, 175MHz): δ 174.2 (C^{20}), 167.5 (C^{16}), 159.5 ($C^{2,11}$), 139.5 ($C^{12,13}$), 137.3 (C^{22}), 136.4 ($C^{4,9}$), 130.7 ($C^{6,7}$), 129.9 (C^{25}), 129.6 (C^{24}), 129.5 ($C^{5,8}$), 129.3 (C^{23}), 127.9 (C^3), 127.9 (C^{10}), 86.7 (C^{17}), 84.0 (C^{17}), 69.1 (C^{cycl}), 67.5 (C^{21}), 61.1 (C^{19}), 60.1 (C^{cycl}), 55.6 (C^{15}), 49.8 (C^{14}), 28.4 (C^{18}), 21.6 (C^1). ESI- MS calcd. for $C_{43}H_{58}N_6O_6$: 754.44. Found: 755.4 $[M+H]^+$ and 378.3 $[M+2H]^{2+}$.

{7-[(6-Methyl-4,5-diaza-3-phenanthryl)methyl]-4,10-bis(tert-butoxycarbonylmethyl)-1,4,7,10-tetraaza-1-cyclododecyl}acetic acid (8)

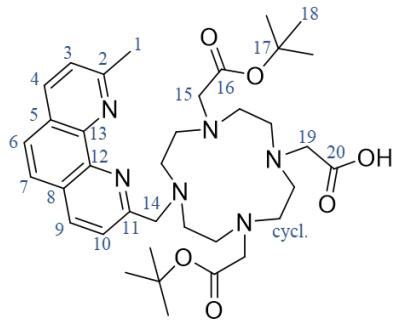

To a solution of **7** (16.6 mg, 0.022 mmol) in MeOH (5 mL), a suspension of Pd/C (1.2 mg, 7% w/w) in MeOH (1 mL) was added. The flask was evacuated and charged with H_2 (1 atm), and then stirred at room temperature for 5 hours. The reaction mixture was filtered, and the solvent removed in vacuo. The resulting oil was purified with reverse phase preparative HPLC (Method

A) with the product eluting at 13.6 min. The fractions containing product were combined and the solvent was removed in vacuo to afford **8** (5.4 mg, 37% yield). ^{1}H NMR (CD_3OD, 700MHz): δ 8.63 (s, 1H, H^{9}), 8.57 (d, 1H H^{4}), 8.09 (d, 1H, H^{6}), 8.05 (d, 1H, H^{7}), 8.00 (s, 1H, H^{3}), 7.89 (d, 1H, H^{10}), 4.93 (s, 2H, H^{14}) 3.96-3.44 (m, 12H, $H^{15,\,cycl}$), 3.29-3.03 (m, 8H, H^{cycl}), 3.02 (s, 3H, H^{1}), 1.20 (s, 18H, H^{18}). ^{13}C{^{1}H} NMR (175 MHz, CD_3OD): δ 172.3 ($C^{16,20}$), 160.5 ($C^{2,11}$), 139.3 ($C^{4,9}$), 130.5 (C^{12}), 129.5 (C^{8}), 129.2 (C^{13}), 128.4 (C^{5}), 127.6 ($C^{6,7}$), 126.6 (C^{3}), 126.5 (C^{10}), 83.5 (C^{17}), 59.4 (C^{cycl}), 55.5 (C^{cycl}), 55.3 ($C^{15,19}$), 52.7 (C^{cycl}), 50.4 (C^{cycl}), 49.5 (C^{14}), 28.3 (C^{18}), 24.2 (C^{1}). ESI- MS calcd. for $C_{36}H_{52}N_6O_6$: 664.39. Found: 665.4 $[M+H]^+$ and 333.4 $[M+2H]^{2+}$

Ditert-butyl 2-(3-{4-[5-(2-{7-[(6-methyl-4,5-diaza-3-phenanthryl)methyl]-4,10-bis(tert-butoxycarbonylmethyl)-1,4,7,10-tetraaza-1-cyclododecyl}acetylamino)pentylamino]-4-oxo-1-tert-butoxycarbonylbutyl}ureido)glutarate (9)

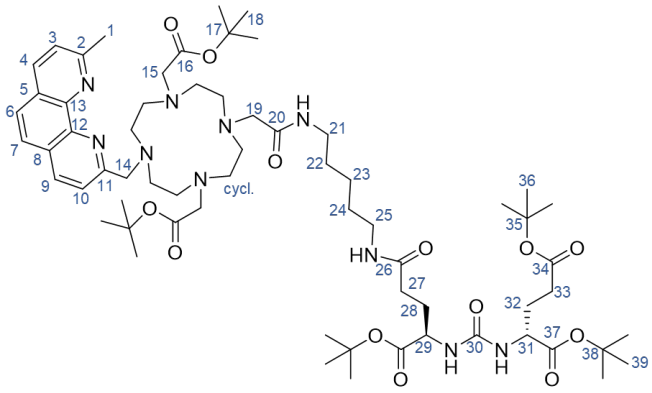

To a solution of **8** (1.5 mg, 0.002 mmol) in DMF (5 mL), DIPEA (0.45 µL, 0.027 mmol) and HBTU (1.3 mg, 0.003 mmol) were added. The mixture was allowed to stir for 15 min and then a solution of ditert-butyl (R)-2-(3-((R)-4-(5-aminopentylamino)-4-oxo-1-tert-butoxycarbonylbutyl)ureido)glutarate[5] (1.3 mg, 0.002 mmol) in DMF (2 mL) was added. The reaction was stirred overnight at room temperature, and the solvent was removed in vacuo. The crude product was purified using reverse phase preparative HPLC (Method A) with the product eluting at 19.2 min (1.6 mg, 58% yield). ^{1}H NMR (CD_3OD, 700MHz): δ 8.71 (s, 1H, H^{9}), 8.61 (s, 1H, H^{4}), 8.24 (s, 1H, H^{3}), 8.12 (q, 2H, $H^{6,7}$), 7.95 (s, 1H, H^{10}), 5.02 (s, 2H, H^{14}), 4.22 (m, 1H, H^{29}), 4.15 (m, 1H, H^{31}), 3.98 (s, 2H, H^{19}), 3.93-2.91 (m, 20H, H^{cycl}), 3.67 (s, 4H, H^{15}), 3.19 (m, 4H, $H^{21,25}$), 3.06 (s, 3H, H^{1}), 2.28 (m, 4H, $H^{27,33}$), 2.08 (m, 2H,

H^{28}), 1.84 (m, 2H, H^{32}), 1.50 (m, 4H, $H^{22,24}$), 1.49, 1.47, 1.32 (s, 45H, $H^{18,36,39}$), 1.38 (m, 2H, H^{23}). ESI- MS calcd. for $C_{64}H_{102}N_{10}O_{13}$: 1218.76. Found: 1219.8 $[M+H]^+$ and 610.6 $[M+2H]^{2+}$

2-(3-{4-[5-(2-{4,10-Bis(carboxymethyl)-7-[(6-methyl-4,5-diaza-3-phenanthryl)methyl]-1,4,7,10-tetraaza-1-cyclododecyl}acetylamino)pentylamino]-1-carboxy-4-oxobutyl}ureido)glutaric acid ((DO2Aphen)-DUPA)

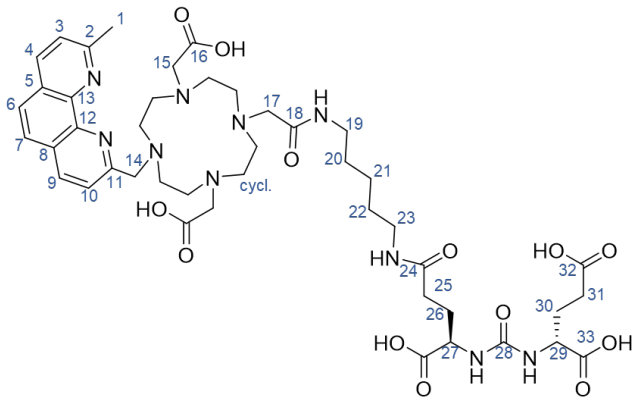

9 (1.6 mg, 0.001 mmol) was dissolved in a solution of 1:2 DCM:TFA (1.5 mL) and stirred at room temperature overnight. The solvent was removed in vacuo, and the product was re-dissolved in H_2O. The solution was then lyophilized to yield **(DO2Aphen)-DUPA** as a white solid (0.8 mg, 65% yield). ^{1}H NMR (CD_3OD, 700MHz): δ 8.98 (d, 1H, H^9), 8.70 (s, 1H, H^4), 8.22 (q, 2H, $H^{6,7}$), 8.12 (d, 2H, $H^{3,10}$), 4.97 (s, 2H, H^{14}), 4.27 (q, 1H, H^{27}), 4.23 (q, 1H, H^{29}), 4.02 (br s, 2H, H^{17}), 3.66- 3.05 (m, 16H, H^{cycl}), 3.51 (m, 4H, H^{15}) 3.16 (s, 3H, H^1), 2.38 (m, 2H, H^{19}), 2.31 (m, 2H, H^{23}), 2.16 (m, 2H, H^{25}), 2.11 (m, 2H, H^{31}), 1.86 (m, 4H, $H^{26,30}$), 1.59 (m, 4H, $H^{20,22}$), 1.42 (m, 2H, H^{21}). HRMS calcd. for $C_{44}H_{62}N_{10}O_{13}$: 938.4498. Found: 939.4560 $[M+H]^+$. HPLC: t_R= 6.3 min (Method C).

1.5 Complexation Protocol

To a solution of ligand dissolved in water, 1 equivalent of $Eu(OTf)_3$ or $Tb(OTf)_3$ salt was added. The pH was adjusted to 7.0-7.5 using 0.1M NaOH. The complex was then purified via SepPak (Waters Sep-Pak C_{18} Plus Short Cartridge, 360 mg Sorbent per Cartridge, 55-105 µm Particle Size). The fractions containing product were pooled and lyophilized, yielding white solids.

Eu(DO3Aphen): product eluted in 90:10 (H_2O: MeCN). HRMS calcd. for $C_{28}H_{33}EuN_6O_6$: 702.1674, 700.1660. Found: 723.1546 $[M+Na]^+$. R_t = 5.7 min (Method C).

[Eu(DO2Aphen)]$^+$: product eluted in 90:10 (H_2O: MeCN). HRMS calcd. for $C_{26}H_{31}EuN_6O_4$: 644.1619. Found: 643.1675 and 645.1692 $[M+H]^+$. R_t = 5.7 min (Method C).

[Eu(DO2Aphen)-DUPA]$^+$: product eluted in 90:10 (H_2O: MeCN). HRMS calcd. for $C_{44}H_{59}EuN_{10}O_{13}$: 1088.3475. Found: 1087.3538 and 1089.3558 $[M+H]^+$. R_t = 6.3 min (Method C).

[Tb(DO2Apic)-DUPA]: product eluted in 90:10 (H_2O: MeCN). HRMS calcd. for $C_{37}H_{54}N_9O_{15}Tb$: 1023.2993. Found: 1024.3060 $[M+H]^+$, 512.6564 $[M+2H]^{2+}$. R_t = 4.4 min (Method C).

2. Supporting Figures, Schemes and Tables

2.1 Characterization of Ligands

2.1.1 NMR Spectra

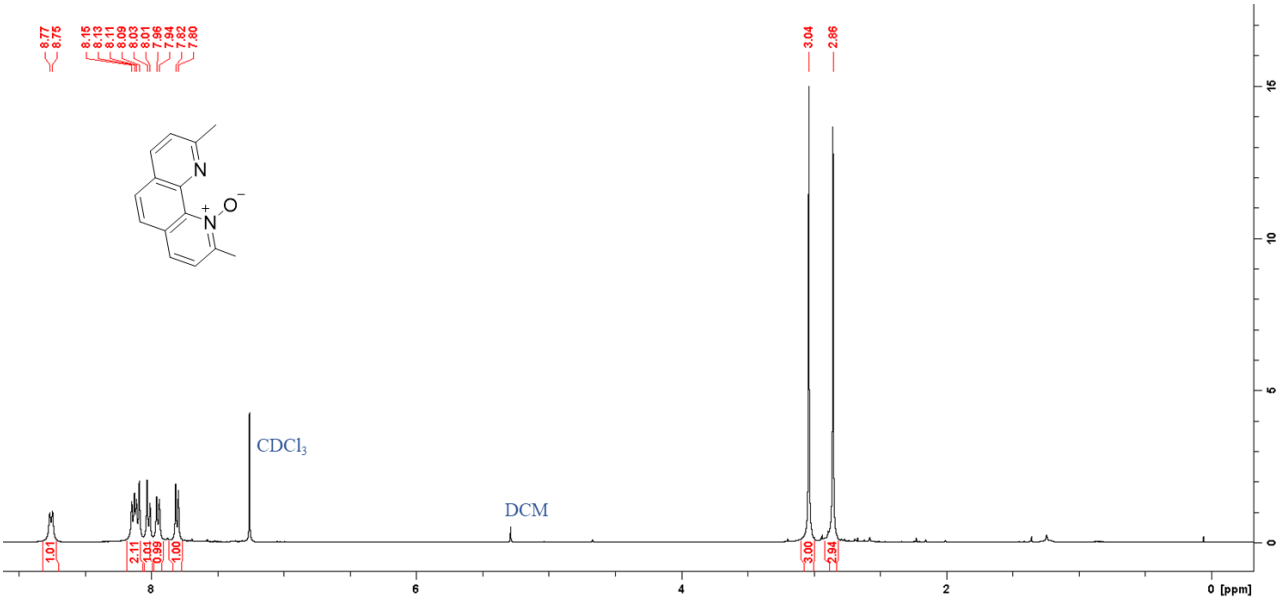

Figure S1. ^{1}H NMR of 2,9-dimethyl-l,10-phenanthroline N-oxide **(1)**. 400 MHz, $CDCl_3$.

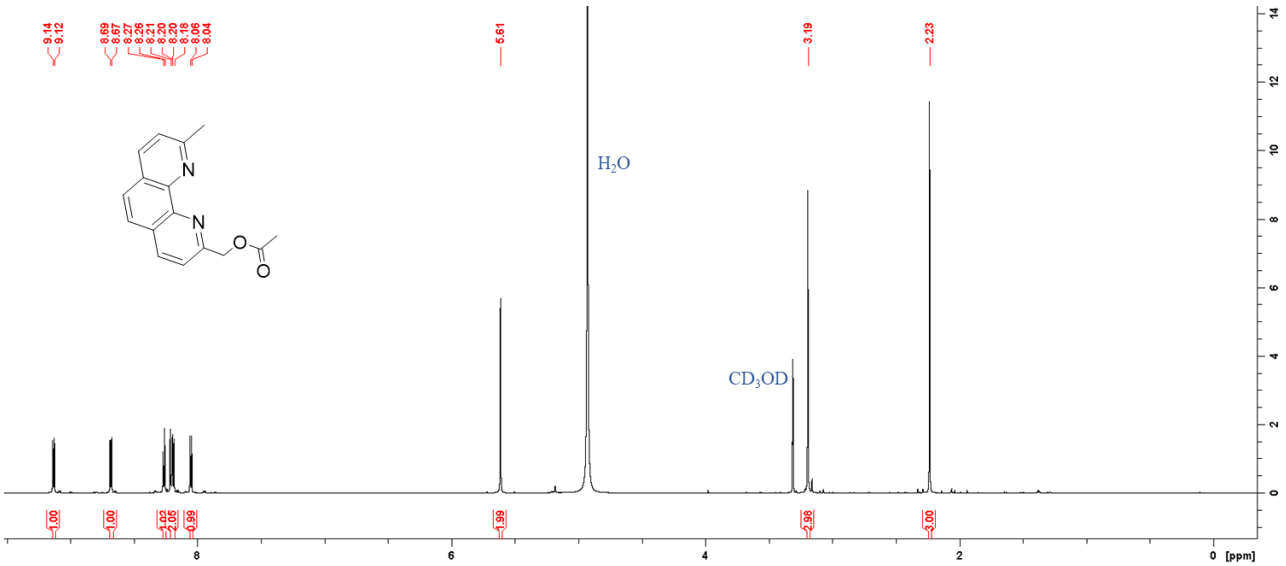

Figure S2. [1]H NMR of 2-(acetoxymethyl)-9-methyl-l,10-phenanthroline **(2)**. 700 MHz, CD_3OD

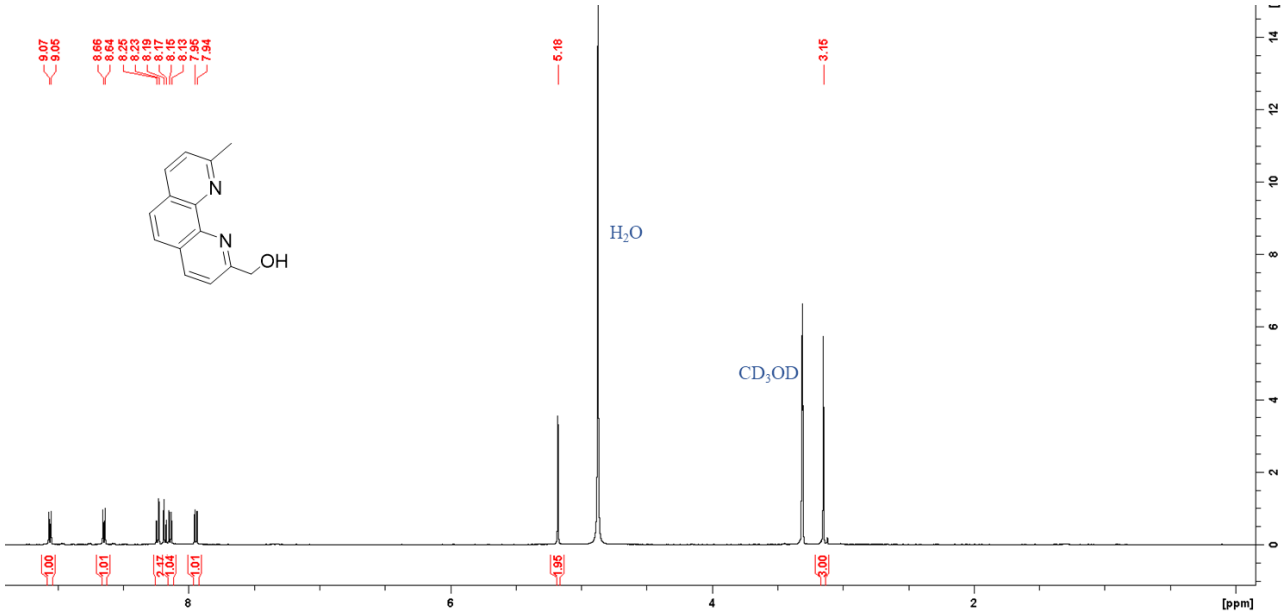

Figure S3. [1]H NMR of 2-(Hydroxymethyl)-9-methyl-l,10-phenanthroline **(3)**. 500 MHz, CD_3OD

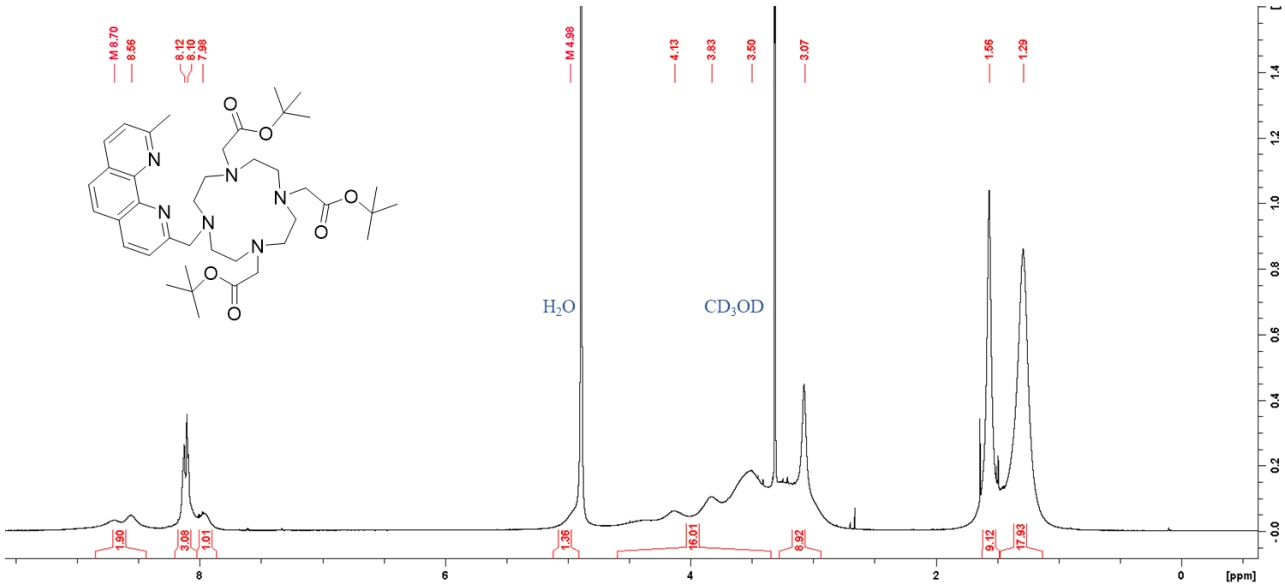

Figure S4. ^{1}H NMR tert-Butyl{4-[(6-methyl-4,5-diaza-3-phenanthryl)methyl]-7,10-bis(tert-butoxycarbonylmethyl)-1,4,7,10-tetraaza-1-cyclododecyl}acetate **(5)**. 700 MHz, CD_3OD

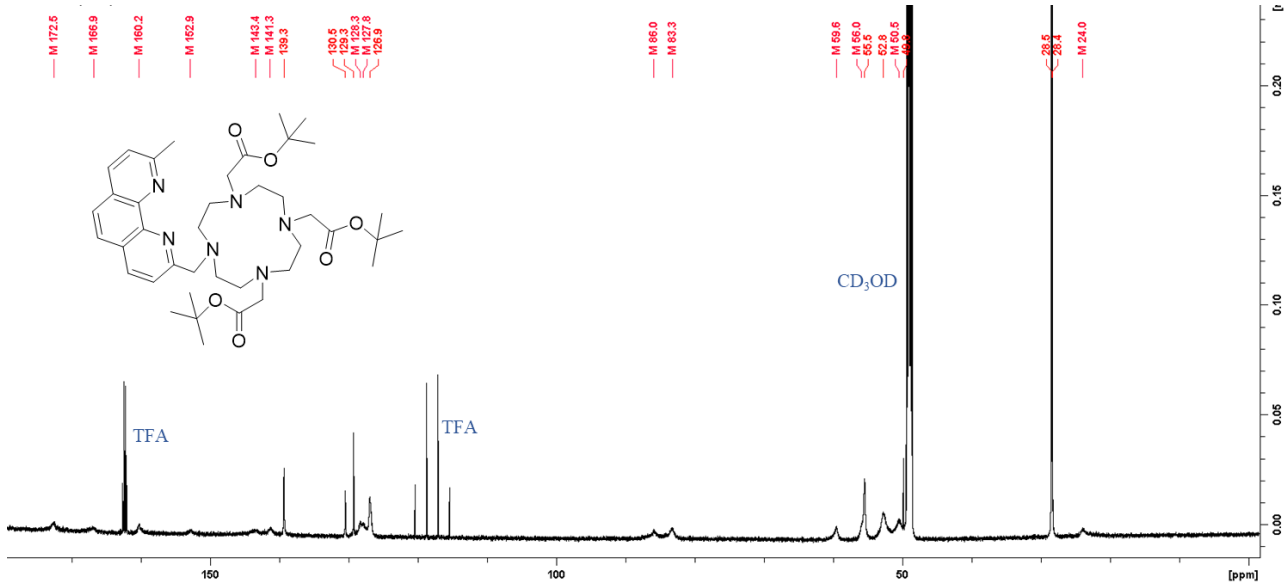

Figure S5. ^{13}C{^{1}H} NMR tert-Butyl{4-[(6-methyl-4,5-diaza-3-phenanthryl)methyl]-7,10-bis(tert-butoxycarbonylmethyl)-1,4,7,10-tetraaza-1-cyclododecyl}acetate **(5)** 700 MHz, CD_3OD

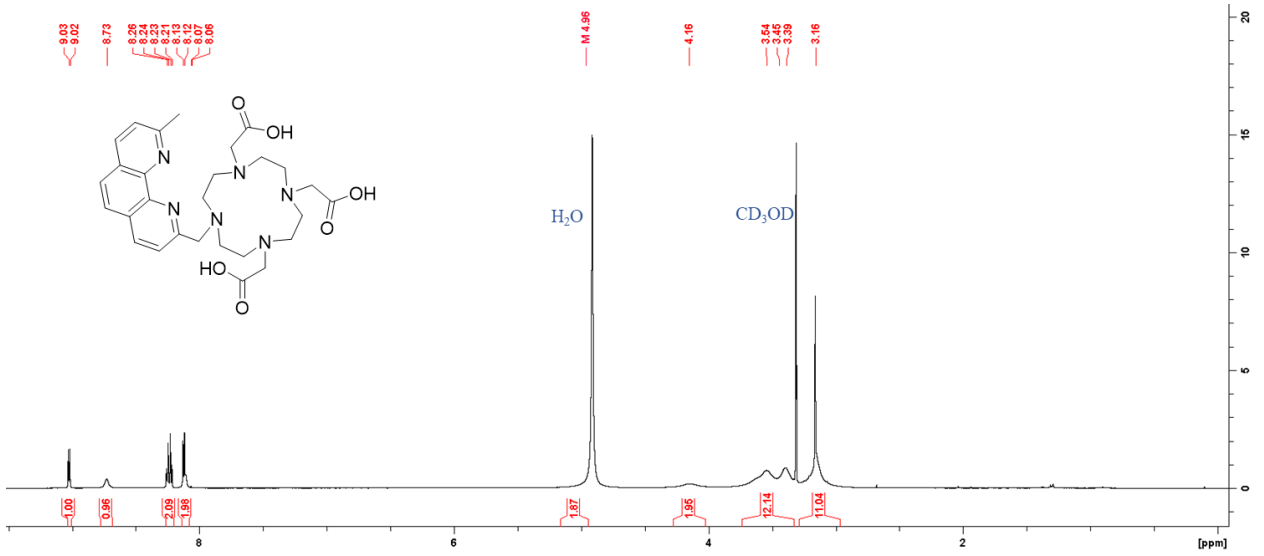

Figure S6. ^{1}H NMR of {4,10-Bis(carboxymethyl)-7-[(6-methyl-4,5-diaza-3-phenanthryl)methyl]-1,4,7,10-tetraaza-1-cyclododecyl}acetic acid, **DO3Aphen**. 700 MHz, CD_3OD

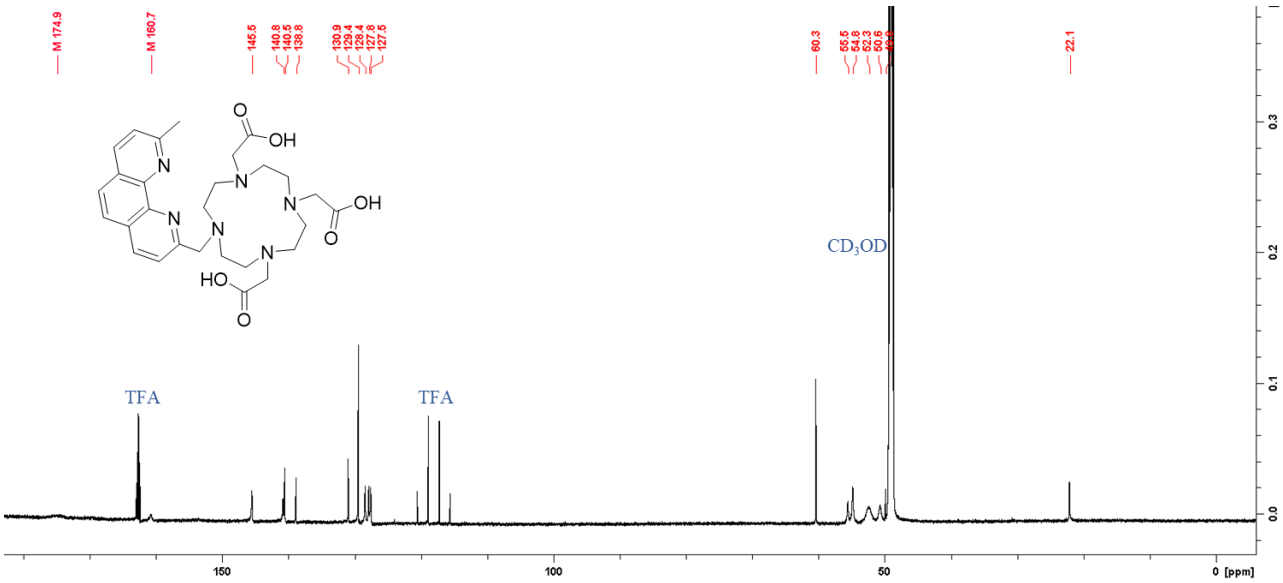

Figure S7. ^{13}C{^{1}H} NMR of {4,10-Bis(carboxymethyl)-7-[(6-methyl-4,5-diaza-3-phenanthryl)methyl]-1,4,7,10-tetraaza-1-cyclododecyl}acetic acid, **DO3Aphen**. 700 MHz, CD_3OD

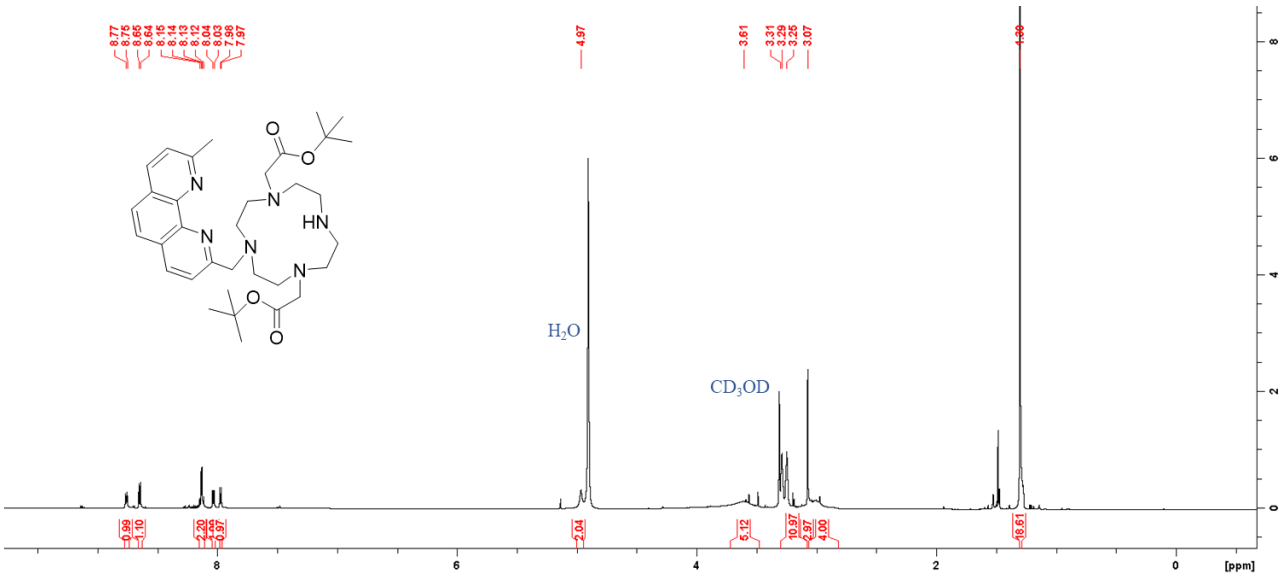

Figure S8. ^{1}H NMR of tert-Butyl {4-[(6-methyl-4,5-diaza-3-phenanthryl)methyl]-7-(tert-butoxycarbonylmethyl)- 1,4,7,10-tetraaza-1-cyclododecyl}acetate **(6)**. 700 MHz, CD_3OD

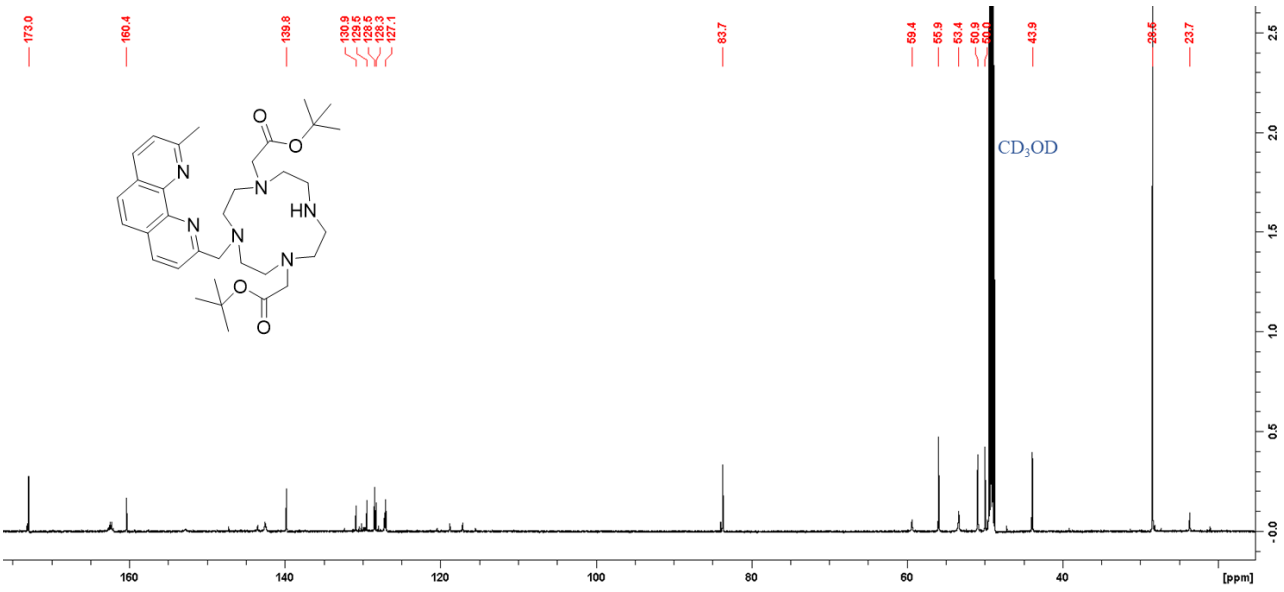

Figure S9. ^{13}C{^{1}H} NMR of tert-Butyl {4-[(6-methyl-4,5-diaza-3-phenanthryl)methyl]-7-(tert-butoxycarbonylmethyl)- 1,4,7,10-tetraaza-1-cyclododecyl}acetate **(6)**. 175 MHz, CD_3OD

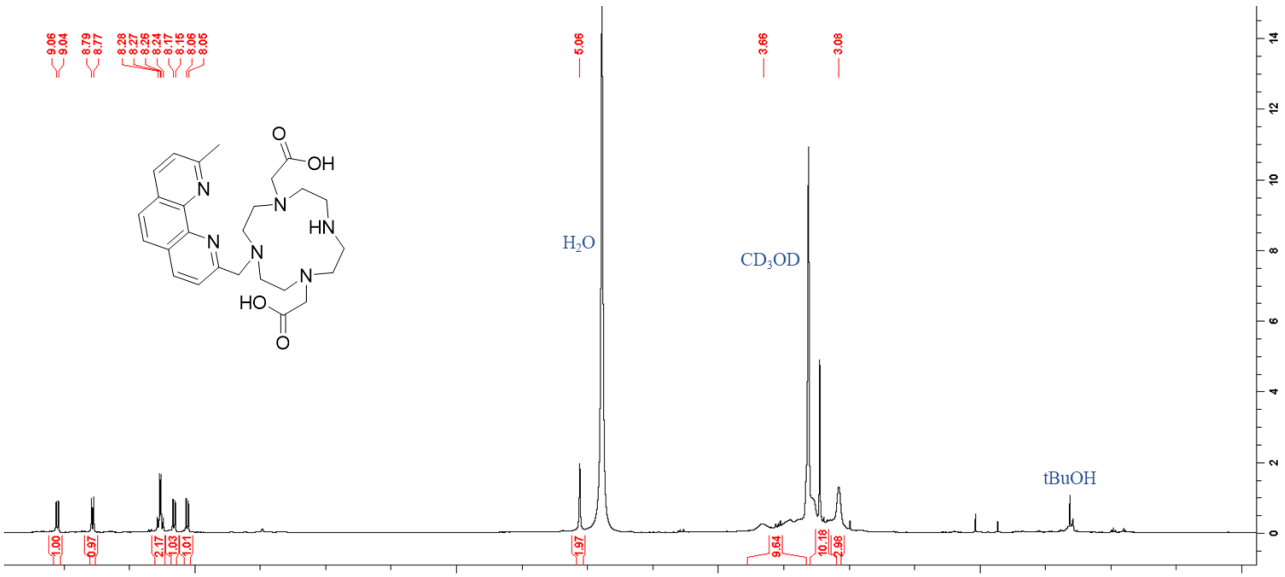

Figure S10. ^{1}H NMR of {7-(Carboxymethyl)-4-[(6-methyl-4,5-diaza-3-phenanthryl)methyl]-1,4,7,10-tetraaza-1-cyclododecyl}acetic acid, **DO2Aphen**. 500 MHz, CD_3OD

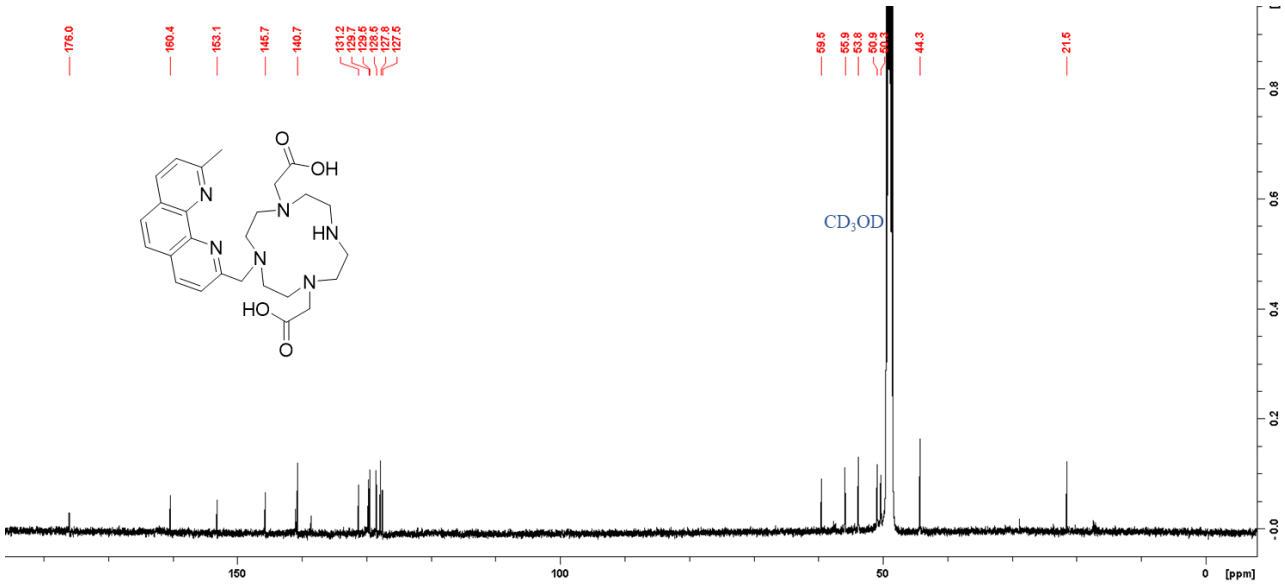

Figure S11. ^{13}C{^{1}H} of {7-(Carboxymethyl)-4-[(6-methyl-4,5-diaza-3-phenanthryl)methyl]-1,4,7,10-tetraaza-1-cyclododecyl}acetic acid, **DO2Aphen**. 125 MHz, CD_3OD

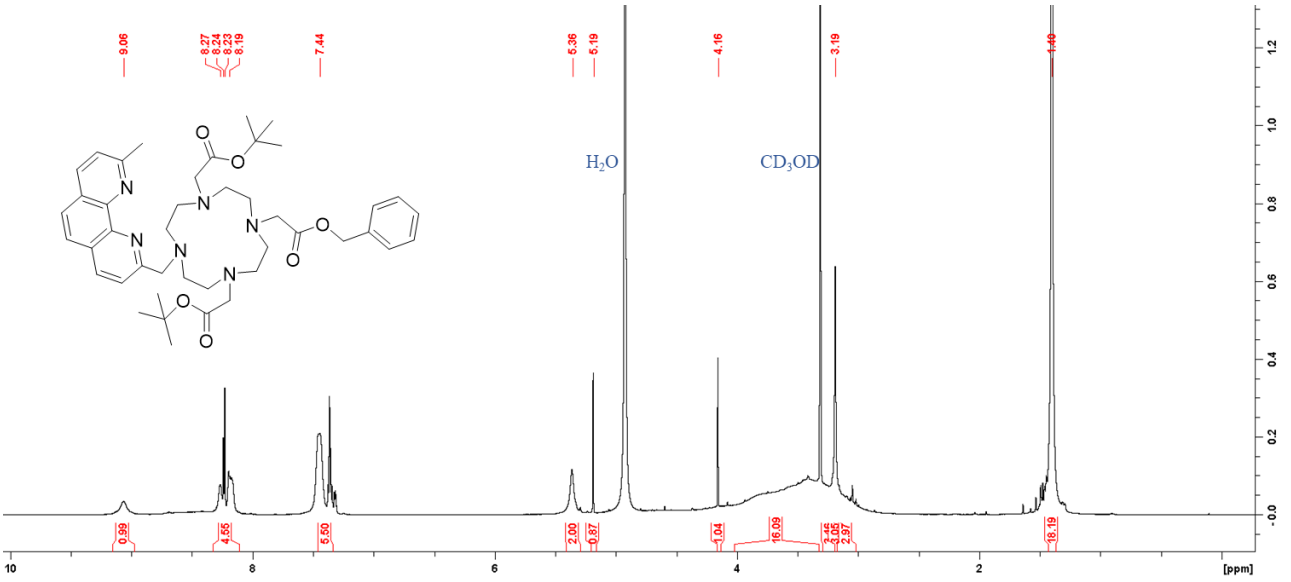

Figure S12. ^{1}H NMR of benzyl{7-[(6-methyl-4,5-diaza-3-phenanthryl)methyl]-4,10-bis(tert-butoxycarbonylmethyl)-1,4,7,10-tetraaza-1-cyclododecyl}acetate **(7)**. 700 MHz, CD_3OD

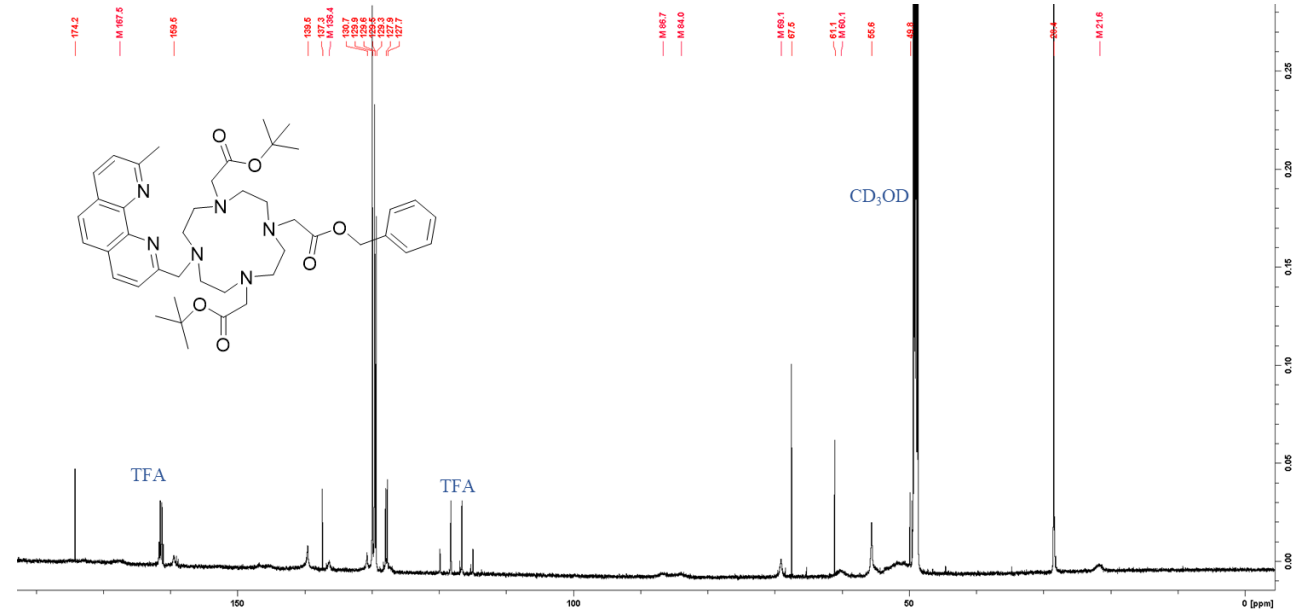

Figure S13. ^{13}C{^{1}H} NMR of benzyl{7-[(6-methyl-4,5-diaza-3-phenanthryl)methyl]-4,10-bis(tert-butoxycarbonylmethyl)-1,4,7,10-tetraaza-1-cyclododecyl}acetate **(7)**. 700MHz, CD_3OD

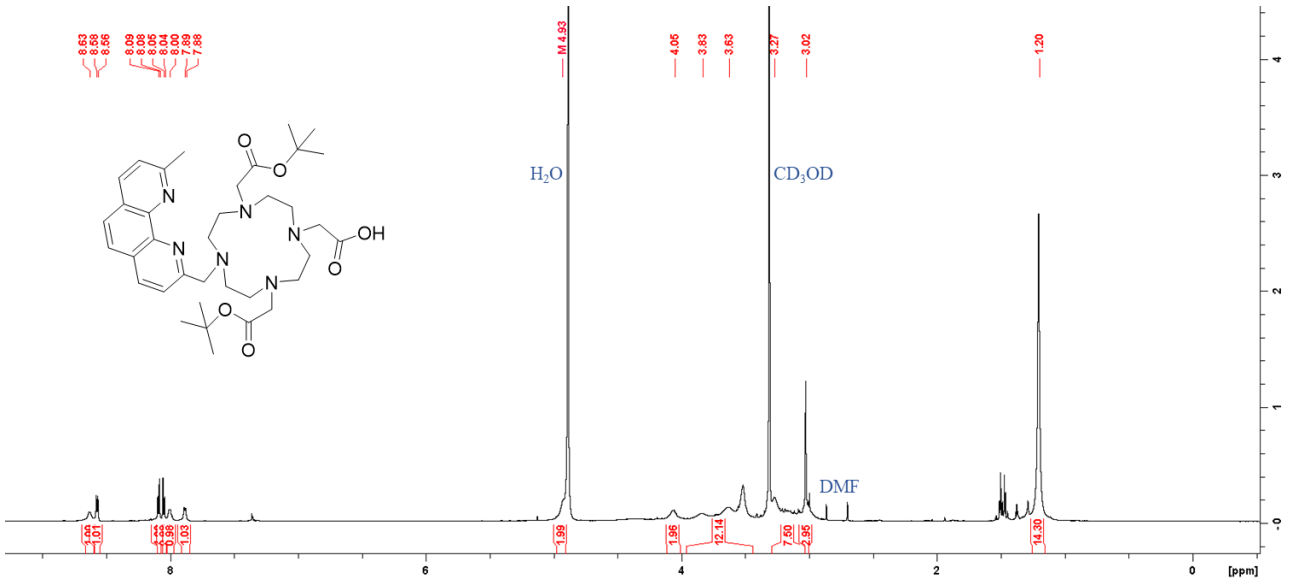

Figure S14. ^{1}H NMR of {7-[(6-Methyl-4,5-diaza-3-phenanthryl)methyl]-4,10-bis(tert-butoxycarbonylmethyl)-1,4,7,10-tetraaza-1-cyclododecyl}acetic acid **(8)**. 700MHz, CD_3OD

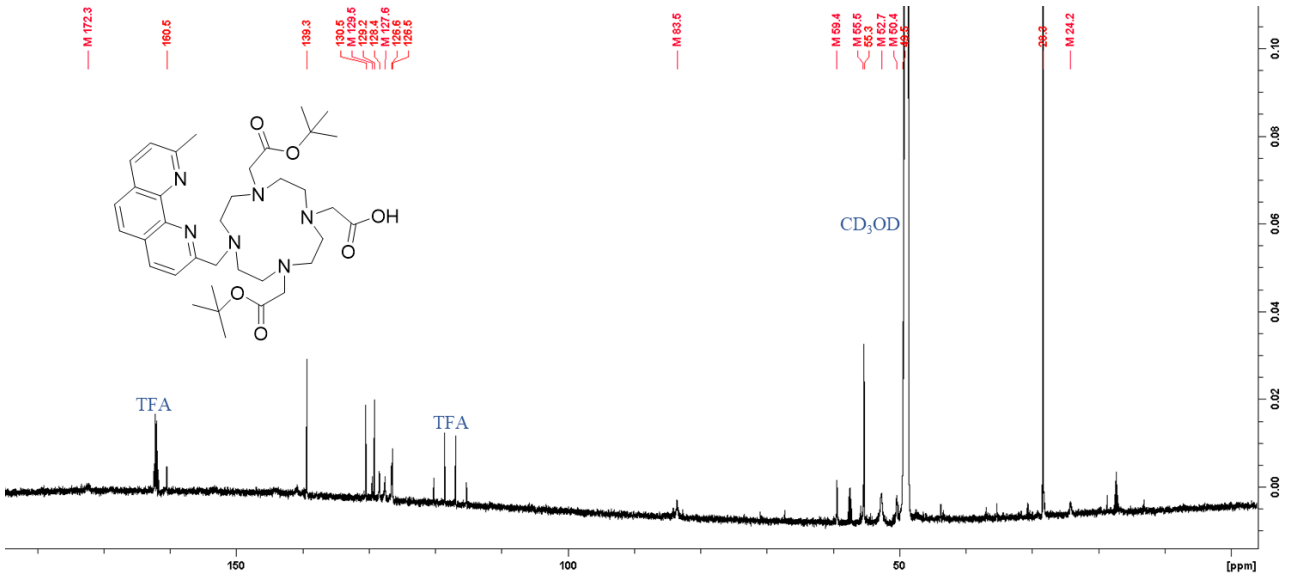

Figure S15. $^{13}C\{^{1}H\}$ NMR of {7-[(6-Methyl-4,5-diaza-3-phenanthryl)methyl]-4,10-bis(tert-butoxycarbonylmethyl)-1,4,7,10-tetraaza-1-cyclododecyl}acetic acid **(8)**. 700MHz, CD_3OD

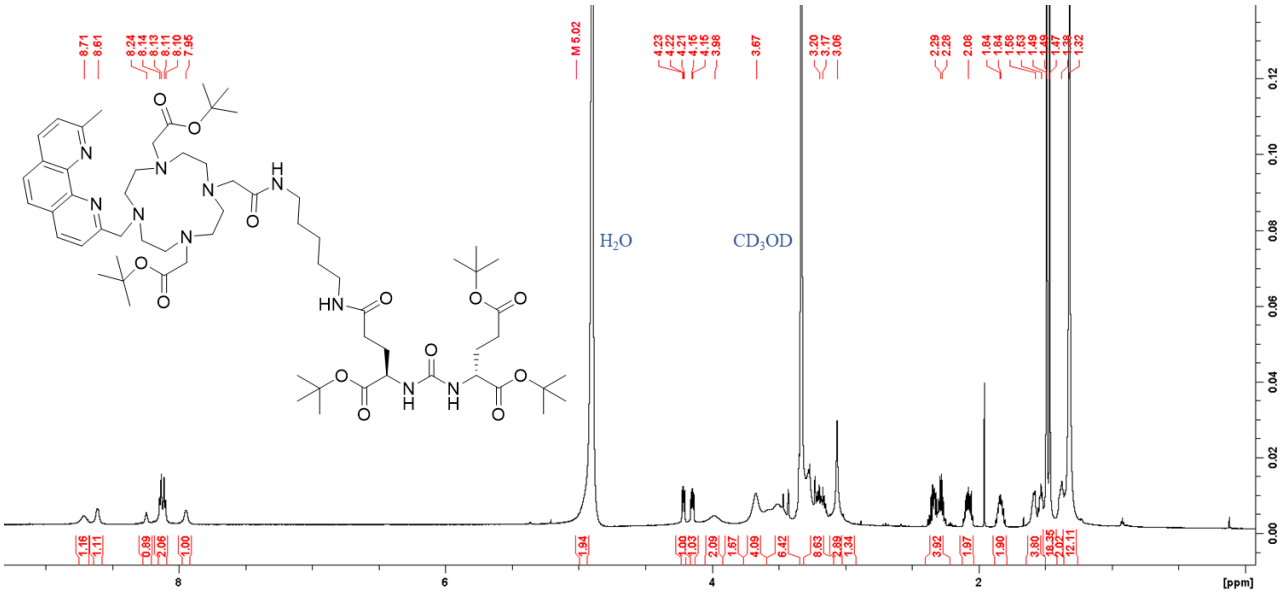

Figure S16. ^{1}H NMR of Ditert-butyl 2-(3-{4-[5-(2-{7-[(6-methyl-4,5-diaza-3-phenanthryl)methyl]-4,10-bis(tert-butoxycarbonylmethyl)-1,4,7,10-tetraaza-1-cyclododecyl}acetylamino)pentylamino]-4-oxo-1-tert-butoxycarbonylbutyl}ureido)glutarate **(9)**. 700MHz, CD_3OD.

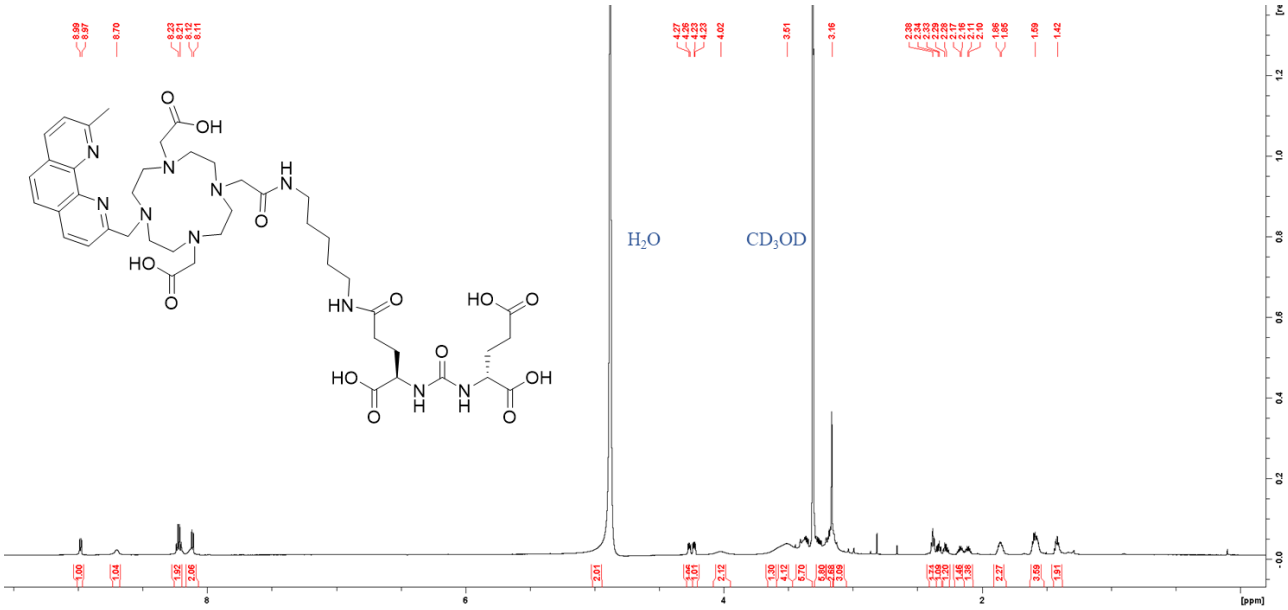

Figure S17. ^{1}H NMR of 2-(3-{4-[5-(2-{4,10-Bis(carboxymethyl)-7-[(6-methyl-4,5-diaza-3-phenanthryl)methyl]-1,4,7,10-tetraaza-1-cyclododecyl}acetylamino)pentylamino]-1-carboxy-4-oxobutyl}ureido)glutaric acid, **DO2Aphen-DUPA**. 700MHz, CD_3OD.

2.1.2 HPLC Chromatograms

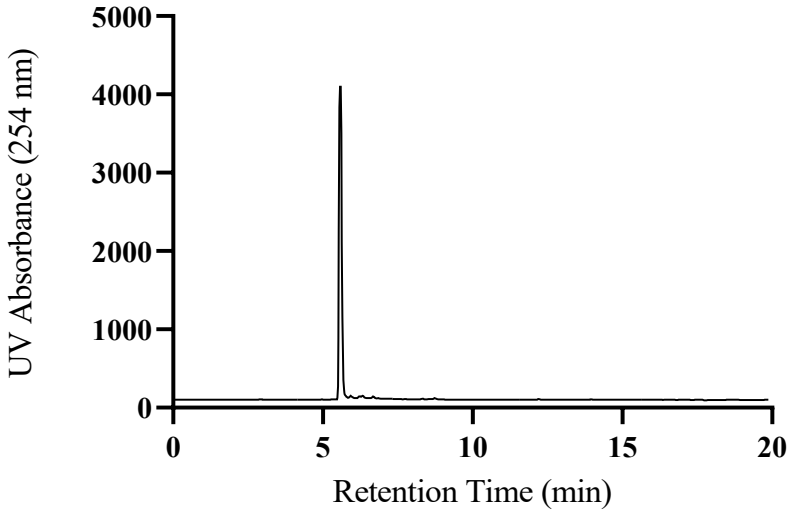

Figure S18. HPLC chromatogram of {4,10-Bis(carboxymethyl)-7-[(6-methyl-4,5-diaza-3-phenanthryl)methyl]-1,4,7,10-tetraaza-1-cyclododecyl}acetic acid, DO3Aphen. Retention time (t_R) = 5.6 min (Method C).

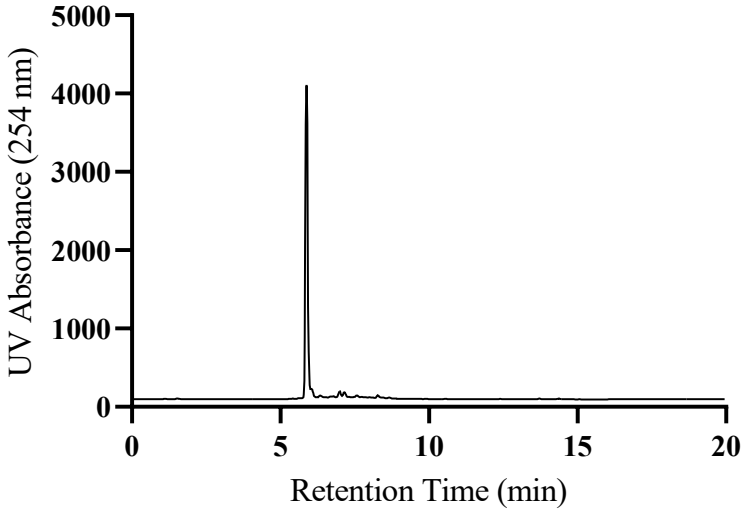

Figure S19. HPLC chromatogram of {7-(Carboxymethyl)-4-[(6-methyl-4,5-diaza-3-phenanthryl)methyl]-1,4,7,10-tetraaza-1-cyclododecyl}acetic acid, DO2Aphen. Retention time (t_R) = 5.7 min (Method C).

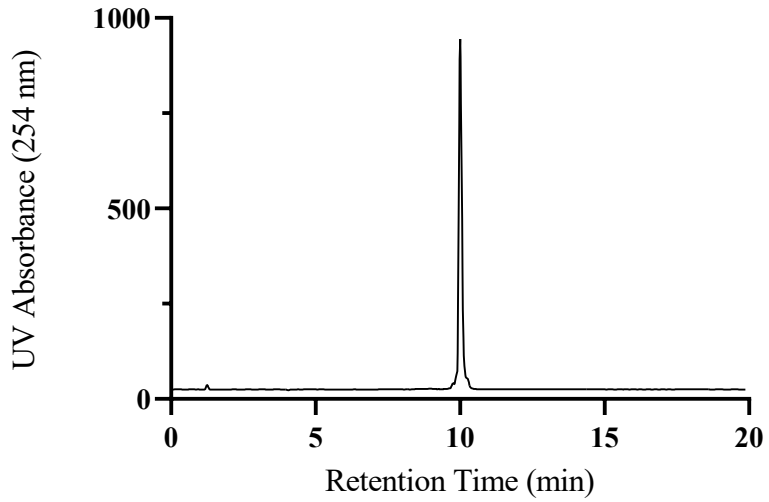

Figure S20. HPLC chromatogram of Ditert-butyl 2-(3-{4-[5-(2-{7-[(6-methyl-4,5-diaza-3-phenanthryl)methyl]-4,10-bis(tert-butoxycarbonylmethyl)-1,4,7,10-tetraaza-1-cyclododecyl}acetylamino)pentylamino]-4-oxo-1-tert-butoxycarbonylbutyl}ureido)glutarate **(9)**. Retention time (t_R) = 10.0 min (Method C).

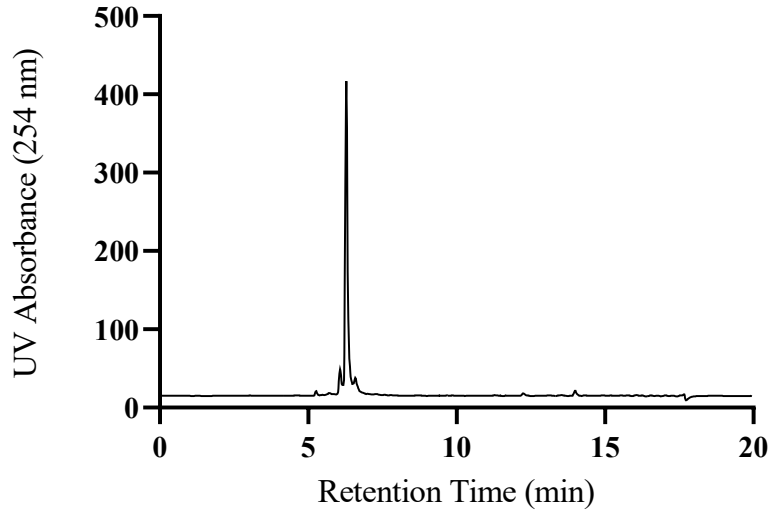

Figure S21. HPLC chromatogram of 2-(3-{4-[5-(2-{4,10-Bis(carboxymethyl)-7-[(6-methyl-4,5-diaza-3-phenanthryl)methyl]-1,4,7,10-tetraaza-1-cyclododecyl}acetylamino)pentylamino]-1-carboxy-4-oxobutyl}ureido)glutaric acid, (DO2Aphen)-DUPA**.** Retention time (t_R) = 6.3 min (Method C).

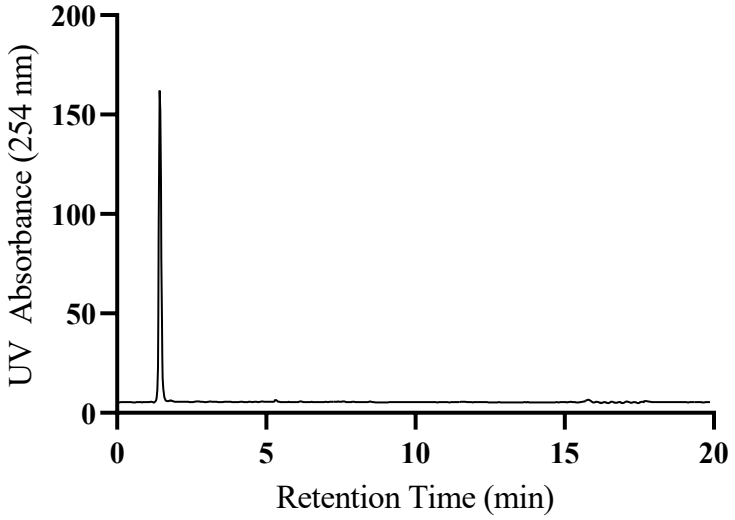

Figure S22. HPLC chromatogram of 2,2',2"-(10-((6-Carboxypyridin-2-yl)methyl)-1,4,7,10-tetraazacyclododecane-1,4,7-triyl)triacetic acid, DO3Apic. Retention time (t_R) = 1.4 min (Method C).

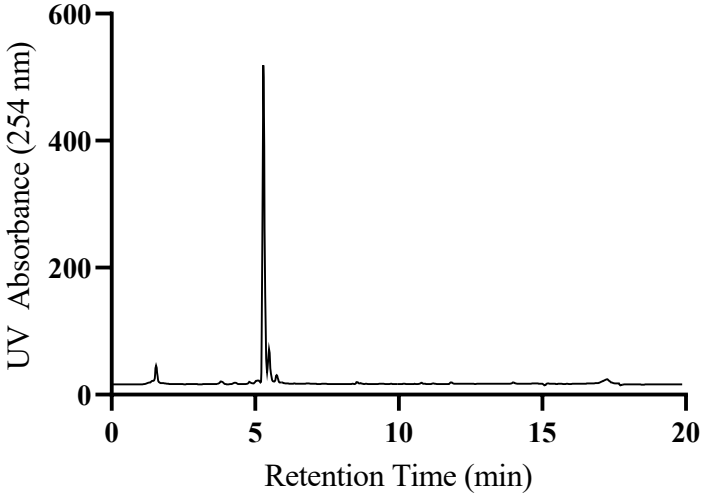

Figure S23. HPLC chromatogram of (13S,17S)-1-(4,10-bis(carboxymethyl)-7-((6-carboxypyridin-2-yl)methyl)-1,4,7,10- tetraazacyclododecan-1-yl)-2,10,15-trioxo-3,9,14,16-tetraazanonadecane-13,17,19-tricarboxylic acid, (DO2Apic)-DUPA. Retention time (t_R) = 5.3 min (Method C).

2.1.3 HRMS Spectra

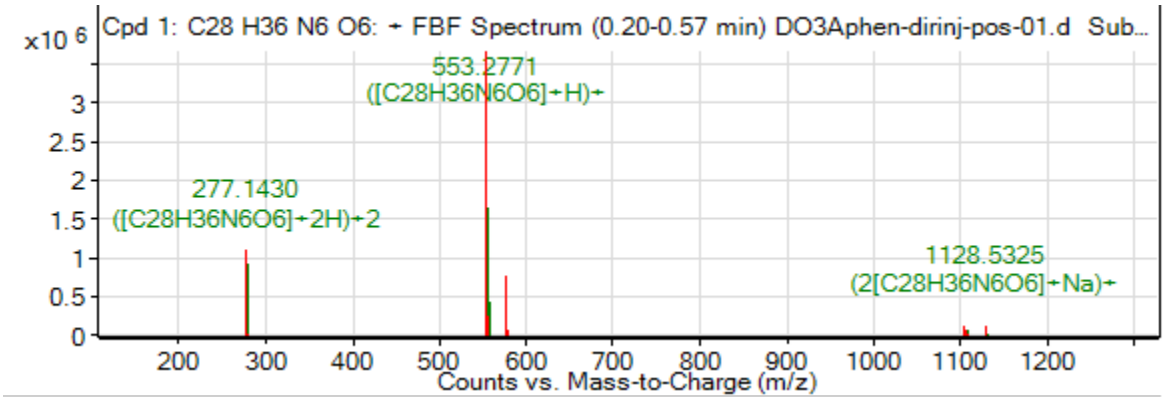

Figure S24. HRMS of {4,10-Bis(carboxymethyl)-7-[(6-methyl-4,5-diaza-3-phenanthryl)methyl]-1,4,7,10-tetraaza-1-cyclododecyl}acetic acid, DO3Aphen. HRMS calcd. for $C_{28}H_{36}N_6O_6$: 552.2969. Found: 553.2771 $[M+H]^+$.

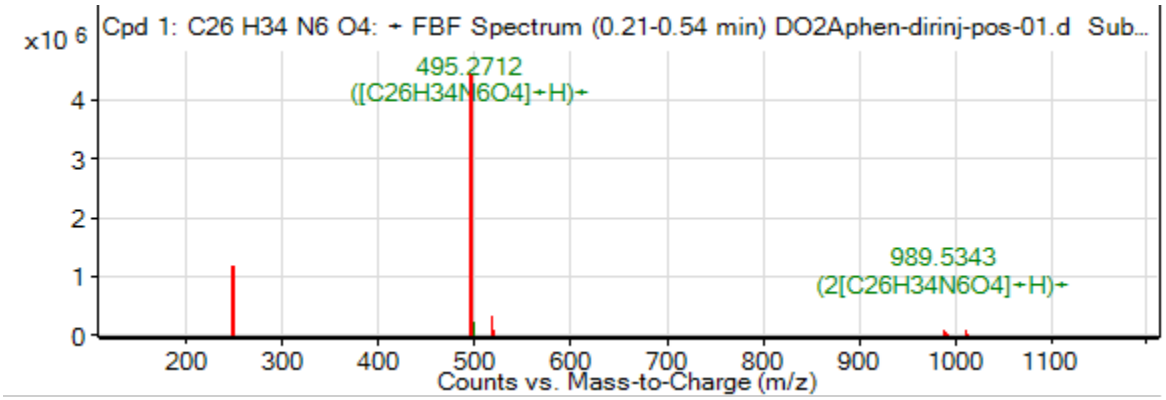

Figure S25. HRMS of {7-(Carboxymethyl)-4-[(6-methyl-4,5-diaza-3-phenanthryl)methyl]-1,4,7,10-tetraaza-1-cyclododecyl}acetic acid, DO2Aphen. HRMS calcd. for $C_{26}H_{34}N_6O_4$: 494.2642. Found: 495.2712 $[M+H]^+$.

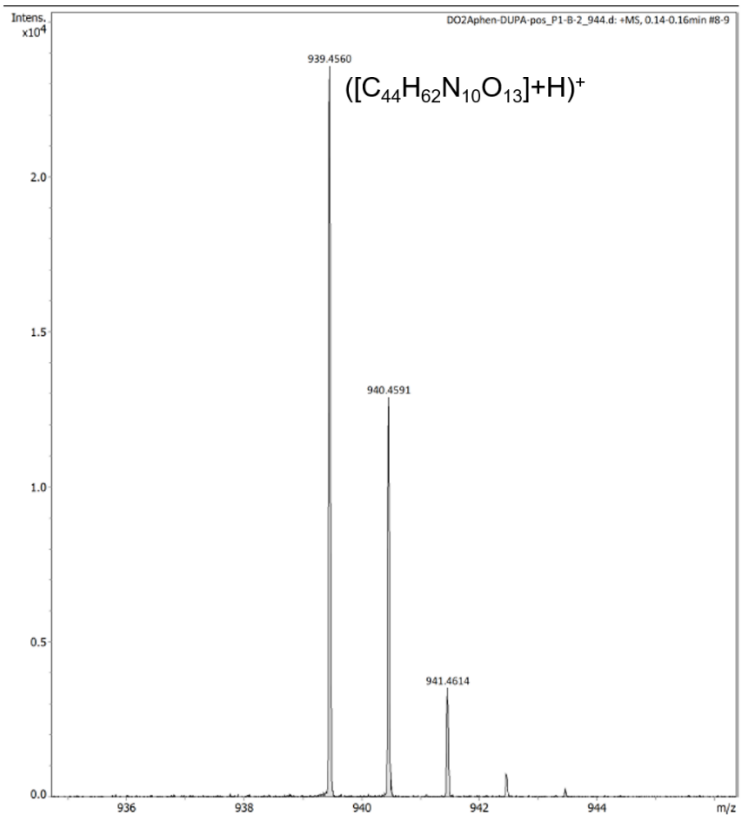

Figure S26. HRMS of 2-(3-{4-[5-(2-{4,10-Bis(carboxymethyl)-7-[(6-methyl-4,5-diaza-3-phenanthryl)methyl]-1,4,7,10-tetraaza-1-cyclododecyl}acetylamino)pentylamino]-1-carboxy-4-oxobutyl}ureido)glutaric acid, (DO2Aphen)-DUPA. HRMS calcd. for $C_{44}H_{62}N_{10}O_{13}$: 938.4498. Found: 939.4560 $[M+H]^+$.

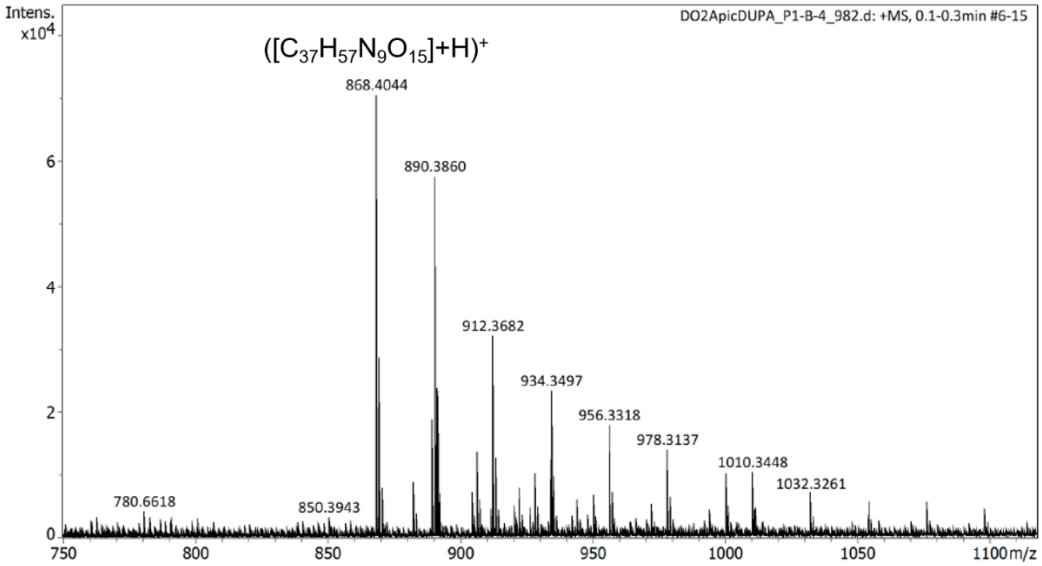

Figure S27. HRMS of (13S,17S)-1-(4,10-bis(carboxymethyl)-7-((6-carboxypyridin-2-yl)methyl)-1,4,7,10- tetraazacyclododecan-1-yl)-2,10,15-trioxo-3,9,14,16-tetraazanonadecane-13,17,19- tricarboxylic acid, (DO2Apic)-DUPA. HRMS calcd. for $C_{37}H_{57}N_9O_{15}$: 867.3974. Found: 868.4044 $[M+H]^+$

2.2 Characterization of Complexes

2.2.1 HPLC Chromatograms

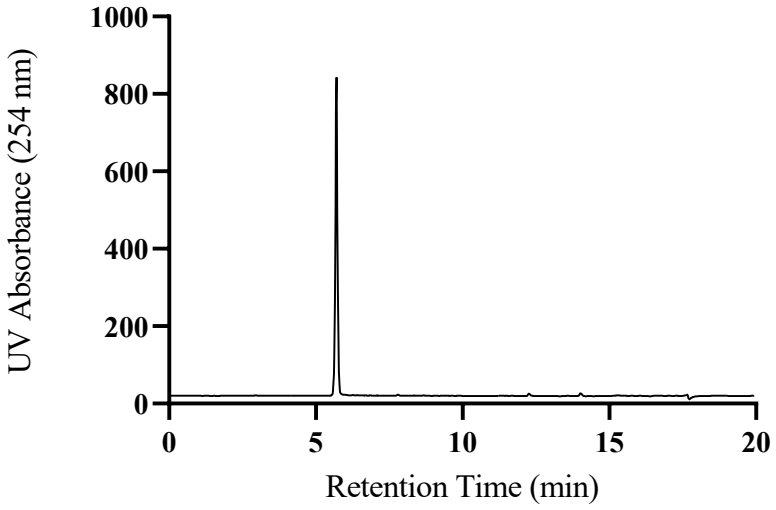

Figure S28. HPLC chromatogram of Eu(DO3Aphen). Retention time (t_R) = 5.7 min (Method C).

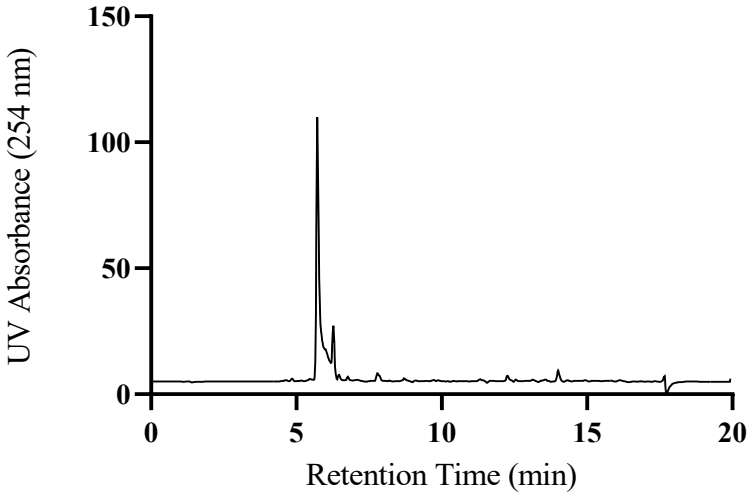

Figure S29. HPLC chromatogram of $[Eu(DO2Aphen)]^+$. Retention time (t_R) = 5.7 min (Method C).

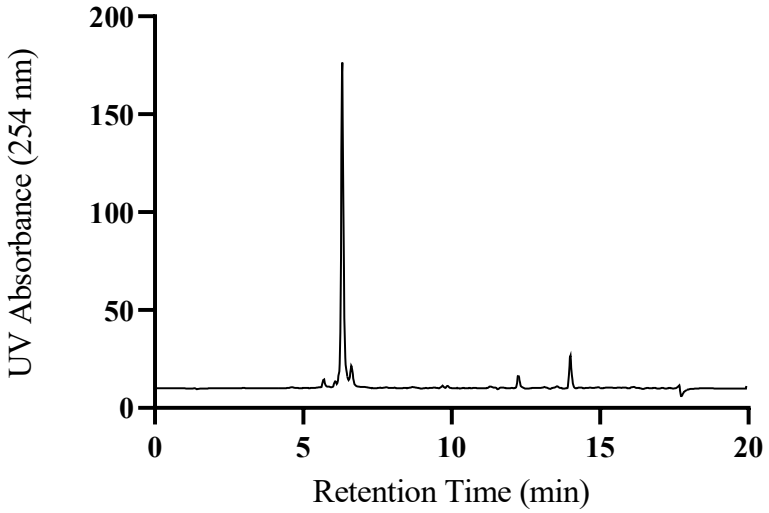

Figure S30. HPLC chromatogram of $[Eu(DO2Aphen)\text{-}DUPA]^{+}$. Retention time ($t_R$) = 6.3 min (Method C).

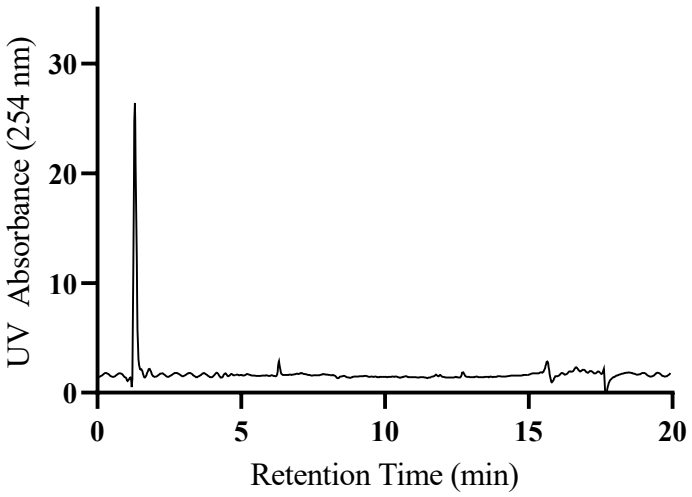

Figure S31. HPLC chromatogram of $[Tb(DO3Apic)]^{-}$. Retention time (t_R) = 1.3 min (Method C).

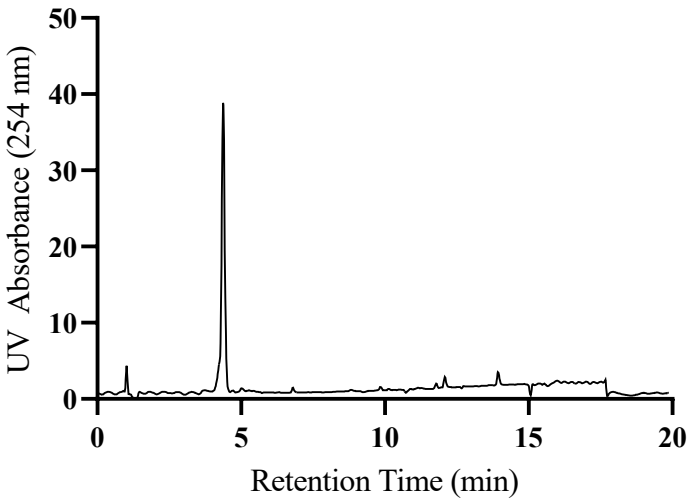

Figure S32. HPLC chromatogram of [Tb(DO2Apic-DUPA)]. Retention time (t_R) = 4.4 min (Method C).

2.2.2 HRMS Spectra

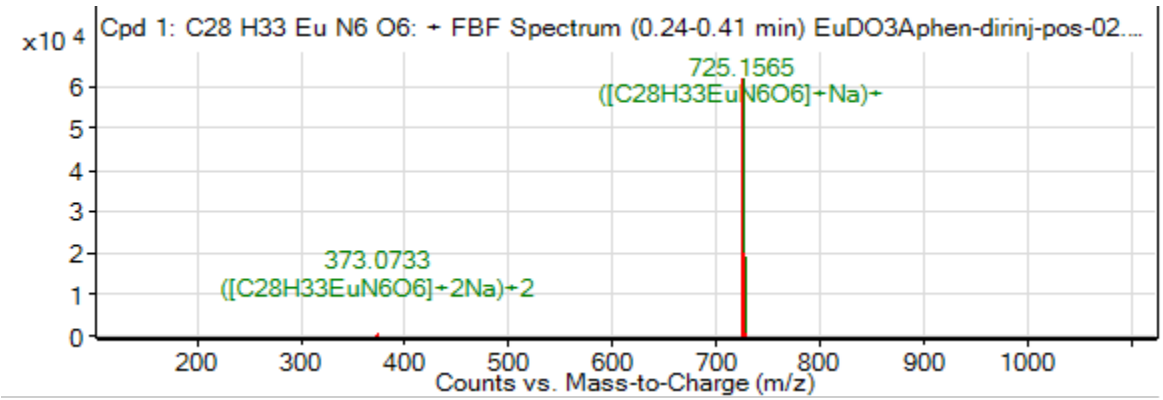

Figure S33. HRMS of [Eu(DO3Aphen)]. HRMS calcd. for $C_{28}H_{33}EuN_6O_6$: 702.1674, 700.1660. Found: 723.1546 $[M+Na]^+$

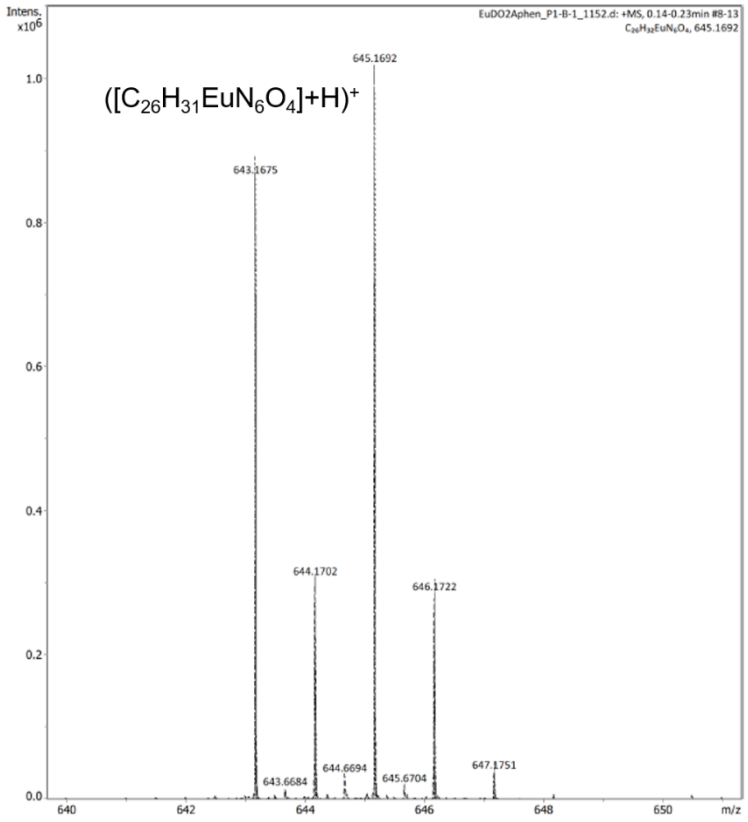

Figure S34. HRMS of $[Eu(DO2Aphen)]^+$. HRMS calcd. for $C_{26}H_{31}EuN_6O_4$: 644.1619. Found: 643.1675 and 645.1692 $[M+H]^+$.

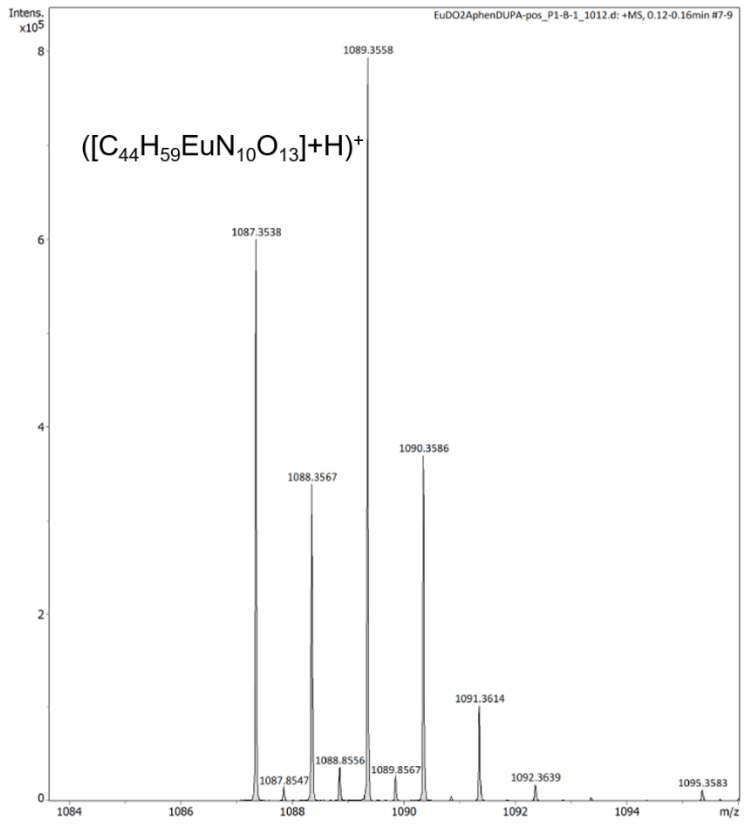

Figure S35. HRMS of [Eu(DO2Aphen)-DUPA]$^{+}$. HRMS calcd. for $C_{44}H_{59}EuN_{10}O_{13}$: 1088.3475. Found: 1087.3538 and 1089.3558 $[M+H]^{+}$.

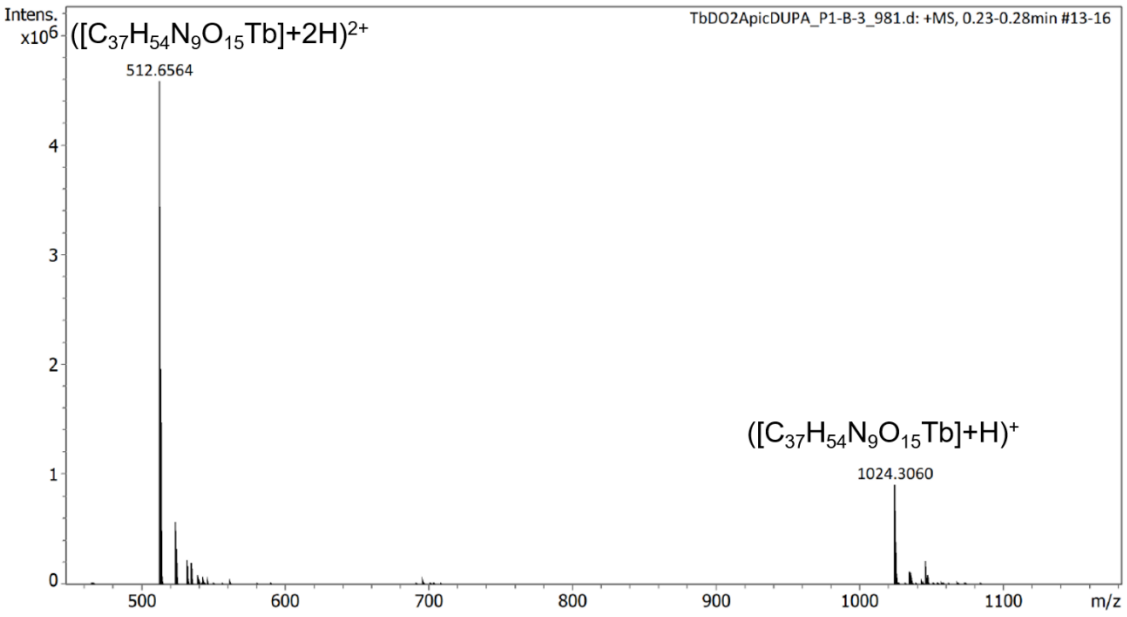

Figure S36. HRMS of [Tb(DO2Apic)-DUPA]. HRMS calcd. for $C_{37}H_{54}N_9O_{15}Tb$: 1023.2993. Found: 1024.3060 $[M+H]^{+}$, 512.6564 $[M+2H]^{2+}$.

2.2.3 Photophysical Characterization Summary

Table S1. Summary of photophysical characterization including, maximum absorbance (λ_{max}) gradient-based Q.Y. (Φ_{Ln}) and gradient, inner-sphere hydration number (q), luminescent lifetimes (τ) determined in H_2O or D_2O and extinction coefficients.

Complex	λ_{max} (nm)	Gradient	Φ_{Ln} [a]	τ, H_2O (ms)	τ, D_2O (ms)	q [b]	ε ($M^{-1}cm^{-1}$)
Eu(DO3Aphen)	283	5199	15%	1.27	1.79	0	23690
$[Eu(DO2Aphen)]^+$	283	1800	5%	0.58	1.82	1.11	31660
$[Eu(DO2Aphen)\text{-}DUPA]^+$	283	3428	10%	1.17	1.73	0	25890
$[Tb(DO3Apic)]^-$ [1]	275	73313	47%	2.83	2.75	0	53926
[Tb(DO2Apic)-DUPA]	275	59250	38%	1.09	1.13	0	37440

[a] Reported with an error of ±10-15%, [b] Reported with an error of ±20%[7]

2.2.4 Absorbance and Emission Profiles

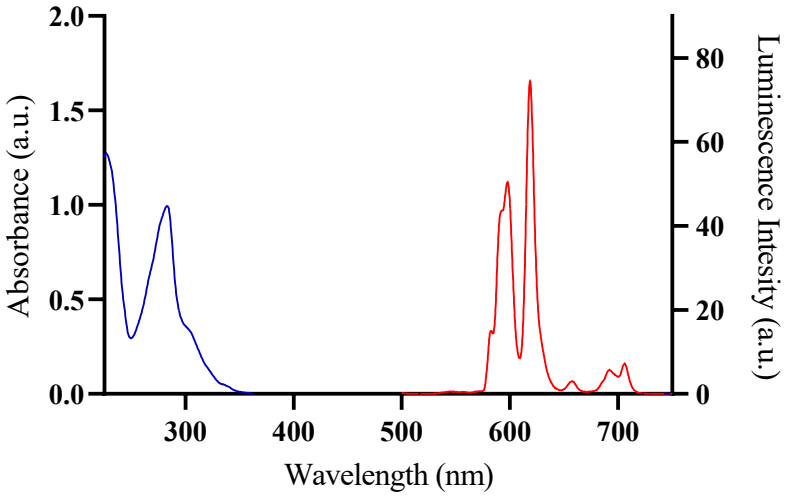

Figure S37. Emission and Absorption Spectra of Eu(DO3Aphen) in 1X DPBS. Absorption is shown in blue and emission is shown in red.

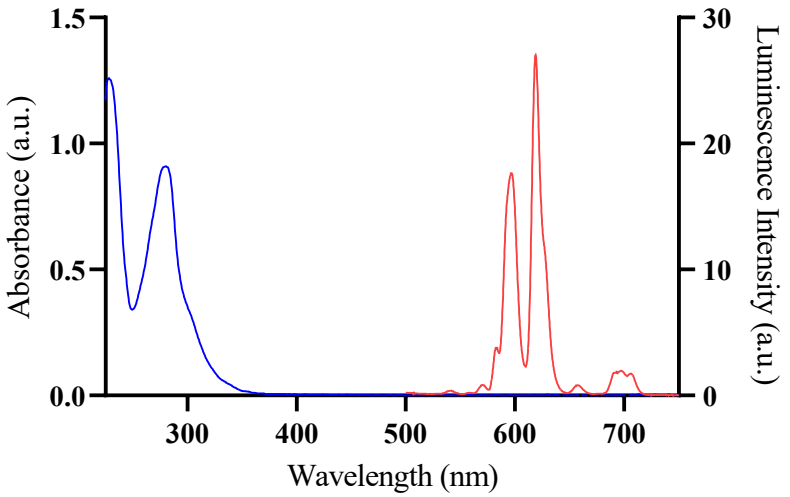

Figure S38. Emission and Absorption Spectra of $[Eu(DO2Aphen)]^+$ in 1X DPBS. Absorption is shown in blue and emission is shown in red.

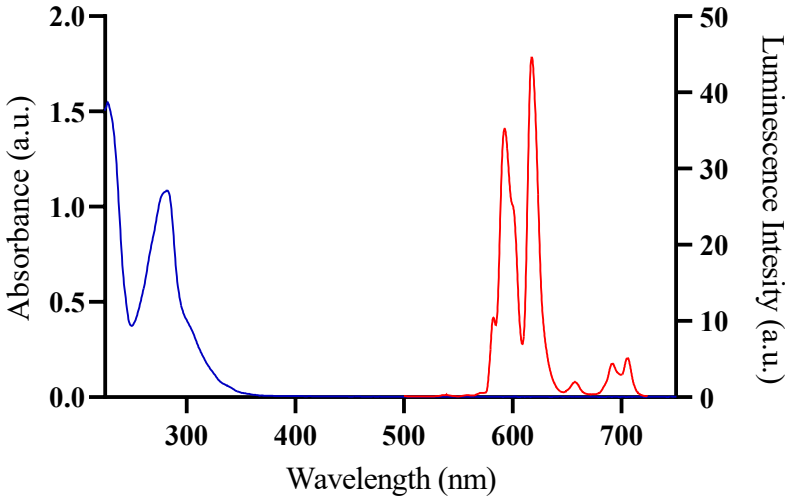

Figure S39. Emission and Absorption Spectra of $[Eu(DO2Aphen)\text{-}DUPA]^+$ in 1X DPBS. Absorption is shown in blue and emission is shown in red.

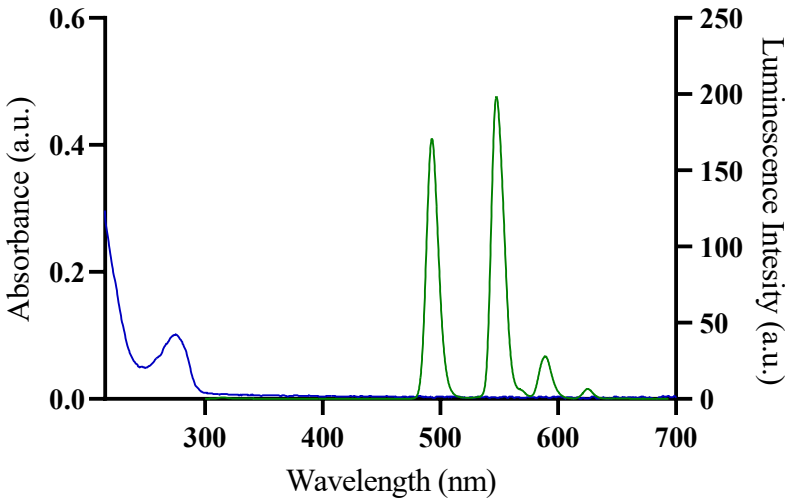

Figure S40. Emission and Absorption Spectra of [Tb(DO2Apic)-DUPA] in 1X DPBS. Absorption is shown in blue and emission is shown in green.

2.2.5 Determination of Quantum Yield

Quantum yield for each complex was determined using the following equation:

$$QY_x = QY_S * \frac{Gradient_X}{Gradient_S}$$

where "S" refers to either the inorganic fluorophore $Ru(bipy)_3$ standard ($\Phi = 0.042$) used for Eu based complexes or $[Tb(DO3Apic)]^-$ ($\Phi = 0.47$) used for Tb based complexes, and "X" is the unknown. The gradient is the slope of the graph of integrated emission intensity versus the peak absorption value for a range of concentrations with absorbance values less than 0.1 (Figures S33 – S36).

Gradients for quantum yield determination were measured by diluting the complexes in 1X DPBS and measuring absorbances ranging 0.01-0.10, followed by measurement of fluorescence emission. Total emission integrals were taken between 576-725 nm for Eu complexes and 450-650 nm for Tb complexes, assuming a Gaussian distribution. The integral of the second-order scattering peak (centered at 564 nm) was subtracted for the Tb complexes. The excitation wavelength employed was 283 nm for Eu and 282 nm for Tb, which centered the scattering peak between the $^5D_4$-$^7F^4$ (544 nm) and $^5D_4$-$^7F_3$ (582 nm) Tb peaks and before the $^5D_0$-$^7F_1$ (590 nm) Eu peak.

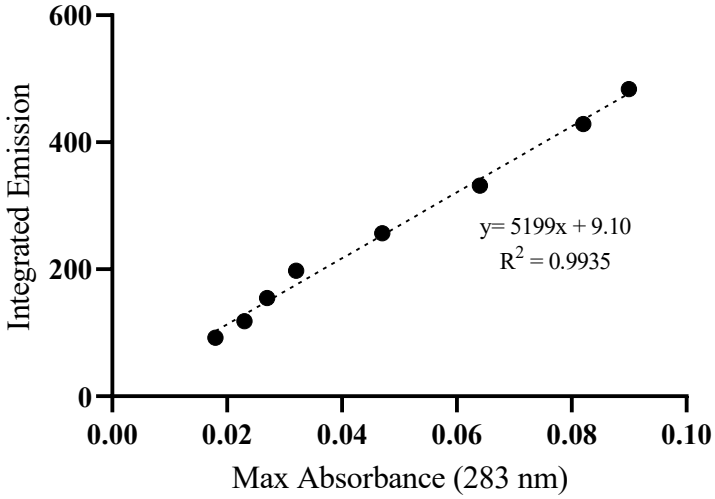

Figure S41. Determination of Gradient Based QY of Eu(DO3Aphen). ($\Phi = 15\%$)

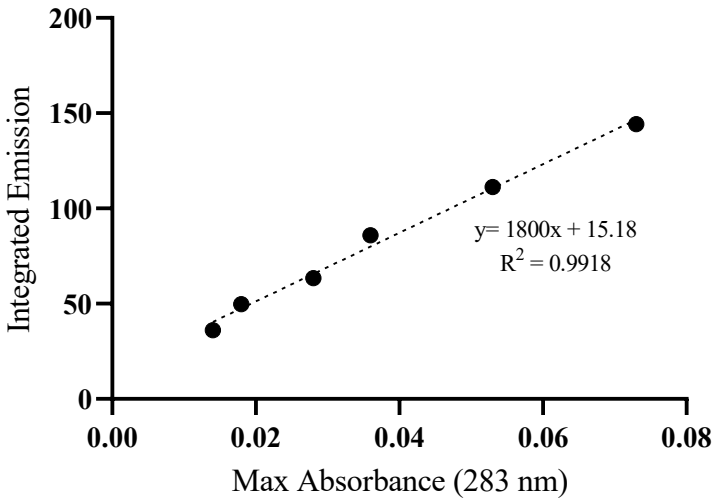

Figure S42. Determination of Gradient Based QY of $[Eu(DO2Aphen)]^{+}$. (Φ = 5%)

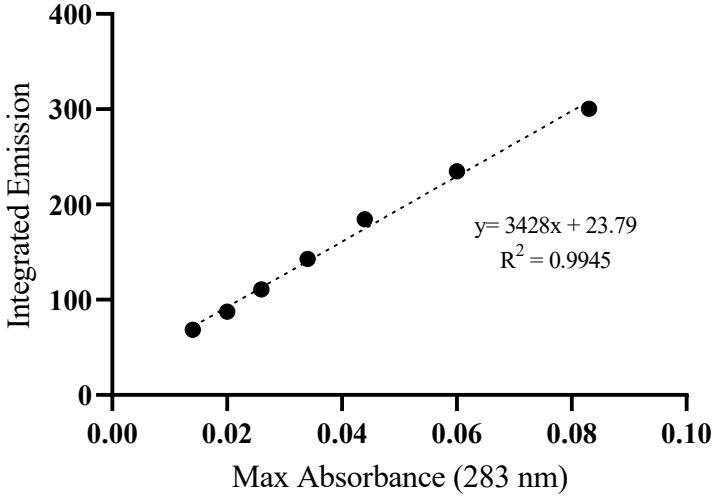

Figure S43. Determination of Gradient Based QY of $[Eu(DO2Aphen)\text{-}DUPA]^{+}$. (Φ = 10%)

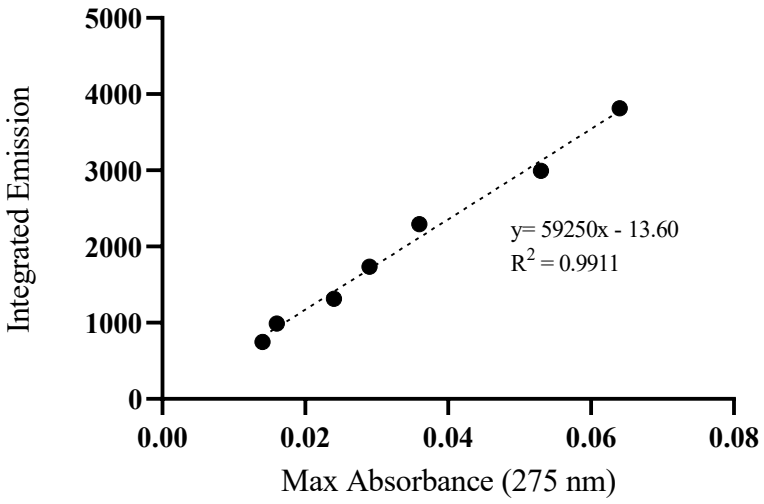

Figure S44. Determination of Gradient Based QY of [Tb(DO2Apic)-DUPA]+. (Φ = 38%)

2.2.6 Extinction Coefficient Determination

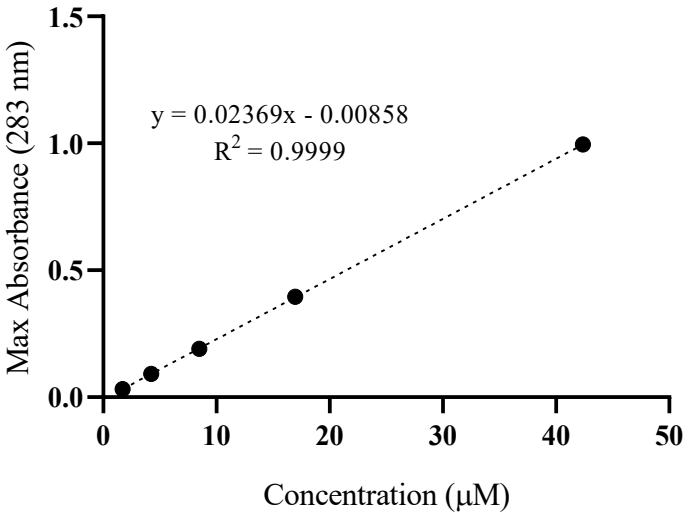

Figure S45. Extinction Coefficient of Eu(DO3Aphen) in 1X DPBS (ε= 23690 M^{-1} cm^{-1})

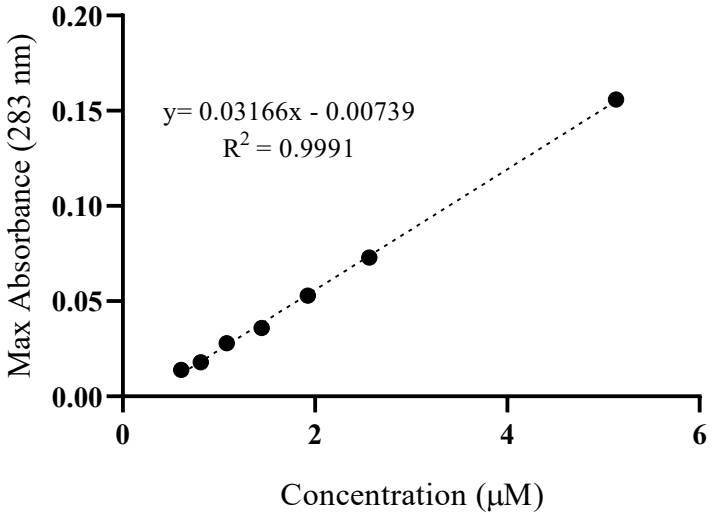

Figure S46. Extinction Coefficient of $[Eu(DO2Aphen)]^{+}$ in 1X DPBS (ε= 31660 M^{-1} cm^{-1})

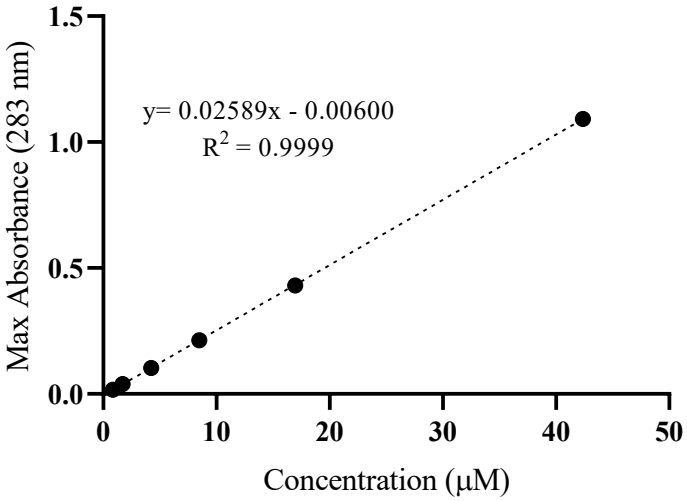

Figure S47. Extinction Coefficient of $[Eu(DO2Aphen)\text{-}DUPA]^{+}$ in 1X DPBS (ε= 25890 M^{-1} cm^{-1})

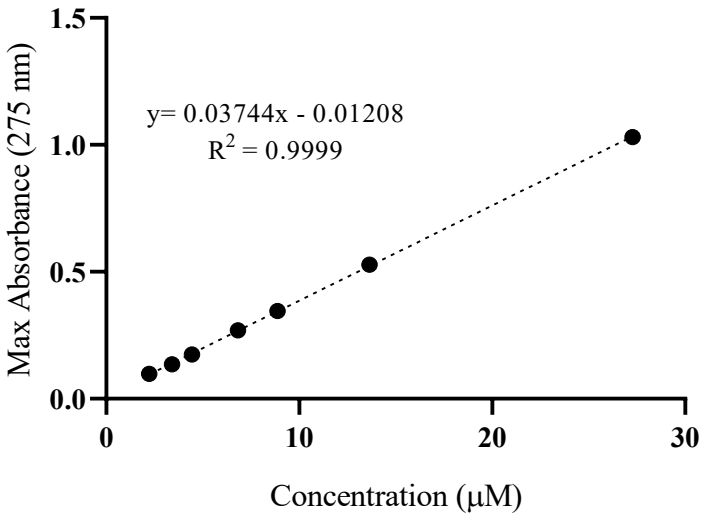

Figure S48. Extinction Coefficient of [Tb(DO2Apic)-DUPA] in 1X DPBS (ε= 37440 M^{-1} cm^{-1})

2.2.7 Lifetime and q Measurements

Lifetime values were extracted by fitting the luminescent decay curves with equation 1.

Equation 1

$$I_t = I_0 * e^{\frac{-x}{\tau}}$$

where I_t is the initial luminescent emission intensity, I_0 is the intensity at time x = 0, and τ is the luminescence lifetime. Data was fit using GraphPad Prism 8.2.0. Q was calculated using Horrocks' method[7], equation 2 shown below.

Equation 2

$$q = A(\frac{1}{\tau_{H_2O}} - \frac{1}{\tau_{D_2O}} - \Delta k)$$

where A is given as 5.0 ms for Tb and 1.2 ms for Eu and Δk is given as 0.06 ms^{-1} for Tb and 0.25 ms^{-1} for Eu. D_2O samples were lyophilized and resuspended in D_2O multiple times before lifetimes were measured.

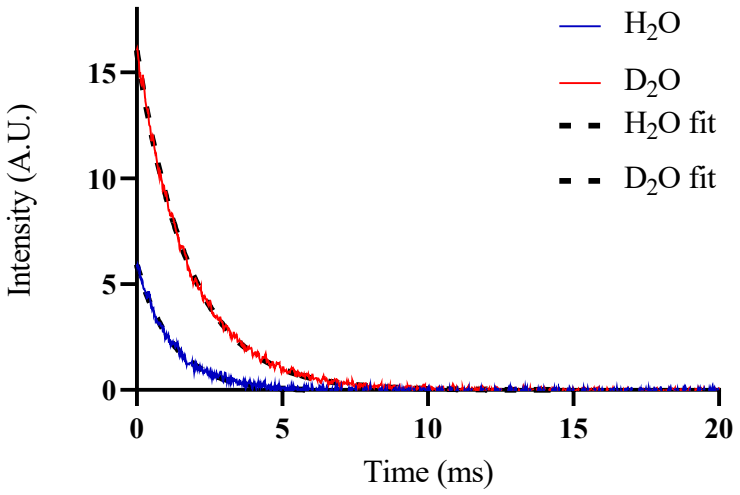

Figure S49. Luminescent lifetime curve for Eu(DO3Aphen). Fits are indicated with dashed black lines.

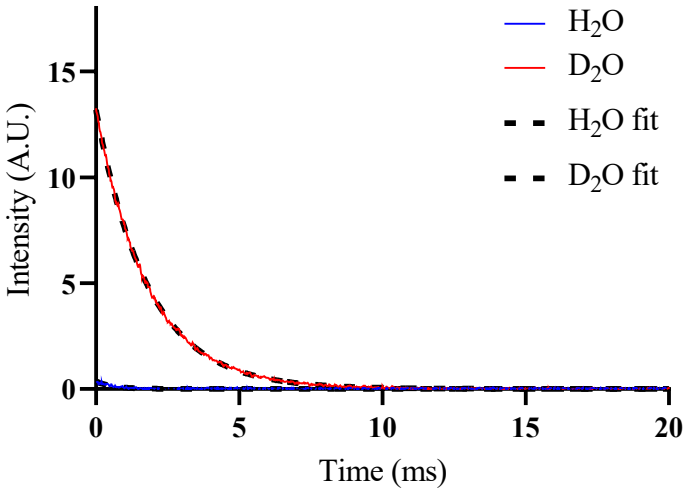

Figure S50. Luminescent lifetime curve for $[Eu(DO2Aphen)]^{+}$. Fits are indicated with dashed black lines.

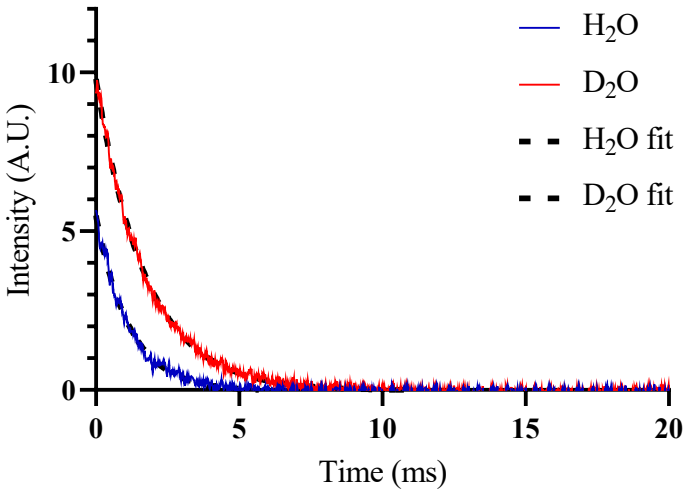

Figure S51. Luminescent lifetime curve for [Eu(DO2Aphen)-DUPA]$^{+}$. Fits are indicated with dashed black lines.

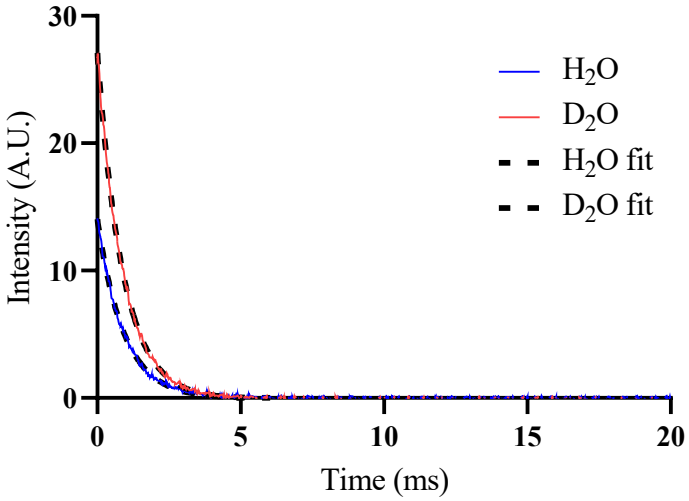

Figure S52. Luminescent lifetime curve for [Tb(DO2Apic)-DUPA]. Fits are indicated with dashed black lines.

2.2.8 Complex Stability: Transchelation Challenge with DTPA

The kinetic inertness of [Eu(DO3Aphen)] and $[Tb(DO3Apic)]^-$ were investigated with a diethylenetriaminepentaacetic acid (DTPA) challenge. The complexes in 1X DPBS (pH 7.4) (Eu(DO3Aphen): 1.85 mM, 20 µL, $[Tb(DO3Apic)]^-$: 0.48 mM, 230 µL) were combined with 1000x excess DTPA (Eu(DO3Aphen): 75 mM, 492 µL, $[Tb(DO3Apic)]^-$: 150 mM, 741 µL) and excess buffer (total volume of each sample: 2 mL), and the UV-VIS spectrum and analytical HPLC (Method C) trace were recorded over 14 days, in triplicate. Standards of complex and free ligand were run alongside the challenge samples. For [Eu(DO3Aphen)] absorbance maximum at 285 nm is characteristic for the complex and at 275 nm is characteristic of the unchelated ligand. The retention times of the complex and uncomplexed ligand were time 5.02 min and 4.85 min, respectively. For [Tb(DO3Apic)] absorbance maximum at 275 nm is characteristic for the complex and at 268 nm is characteristic of the unchelated ligand. The retention times of the complex and uncomplexed ligand were time 1.55 min and 1.52 min, respectively.

To assess the kinetic inertness under slightly acidified conditions, DTPA challenges were also conducted at pH 6.5. The complexes in DI water [Eu(DO3Aphen)]: 26.11µM, 20 µL, $[Tb(DO3Apic)]^-$: 11.96 µM, 80 µL) were combined with 1000x DTPA [Eu(DO3Aphen)]: 198.5 mM, 91 µL, $[Tb(DO3Apic)]^-$: 198.5 mM, 42 µL) in ammonium formate buffer (10 mM, pH 6.5, total volume of each sample: 200 µL). Complexes in triplicate were monitored via analytical HPLC (Method D) over 24 hours with standards of each complex and ligand run for comparison.

R_t [Eu(DO3Aphen)]: 3.27 min; DO3Aphen: 1.36 min; $[Tb(DO3Apic)]^-$:1.49 min; DO3Apic: 0.88 min. DTPA: 0.75 min.

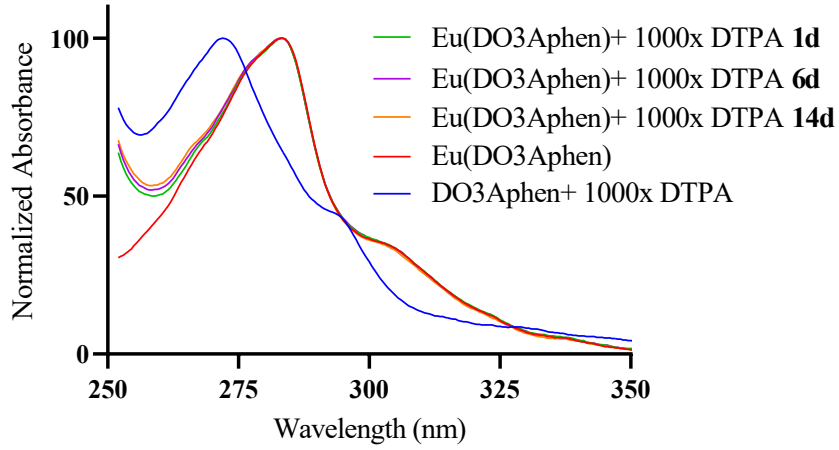

Figure S53. Stability of [Eu(DO3Aphen)] in the presence of a competing ligand at pH 7.4. UV-vis spectra of the samples were acquired at various time points over a two-week time period.

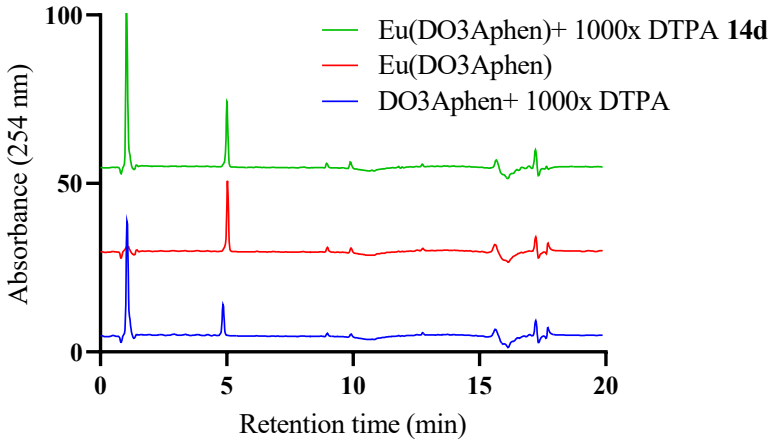

Figure S54. Stability of [Eu(DO3Aphen)] in the presence of a competing ligand at pH 7.4. HPLC chromatograms were acquired at various time points over a two-week time period. (Method C)

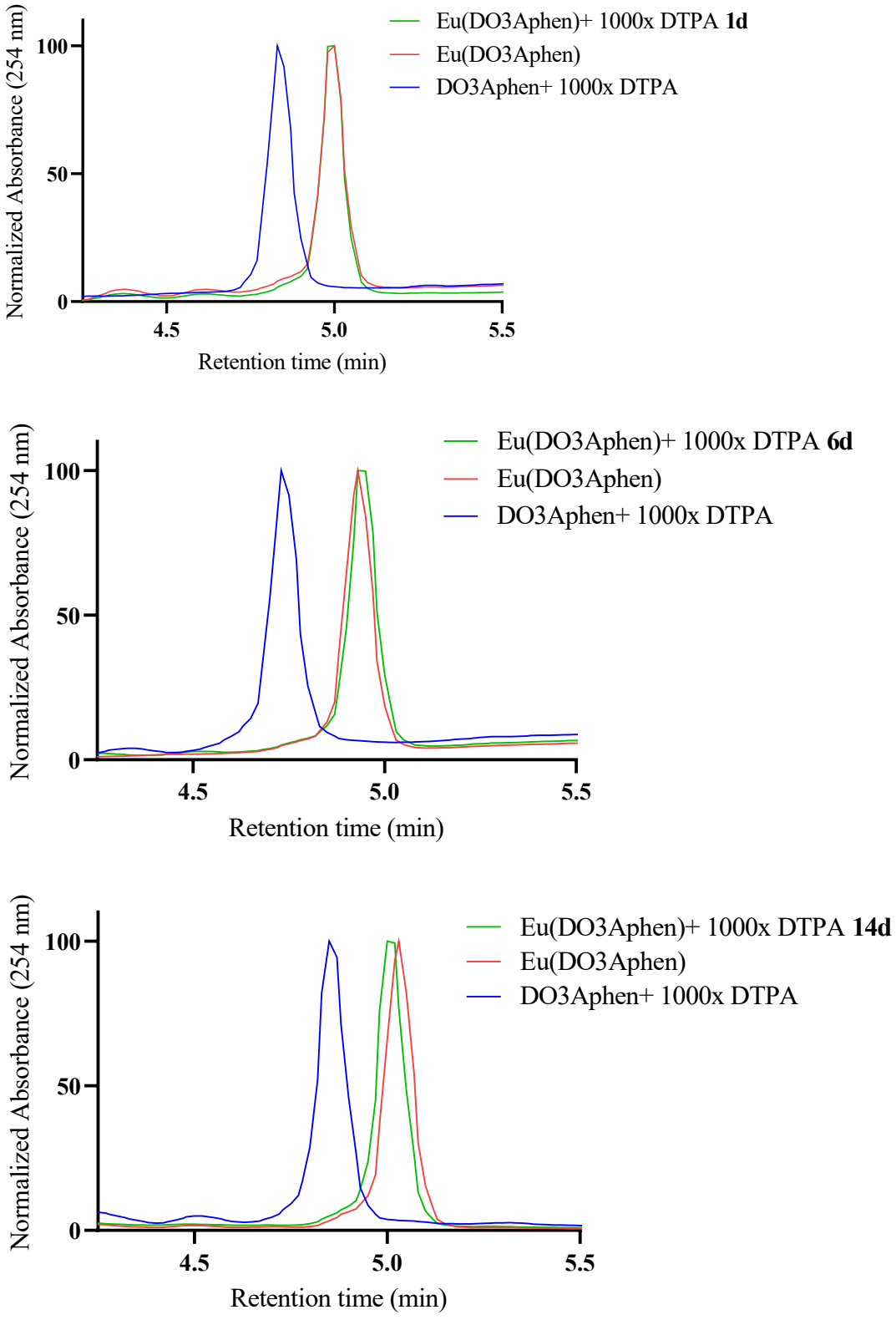

Figure S55. Stability of [Eu(DO3Aphen)] in the presence of a competing ligand at pH 7.4. HPLC chromatograms were acquired at various time points over a two-week time period. (Method C)

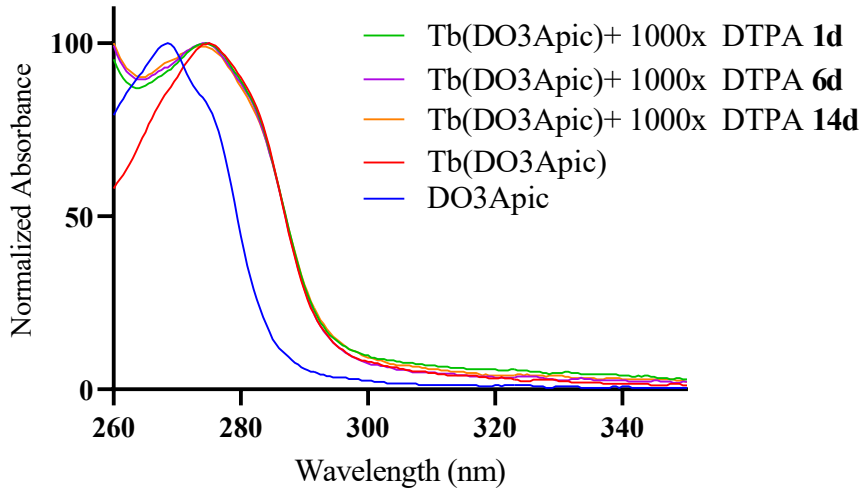

Figure S56. Stability of $[Tb(DO3Apic)]^-$ in the presence of a competing ligand at pH 7.4. UV-vis spectra of the samples were acquired at various time points over a two-week time period.

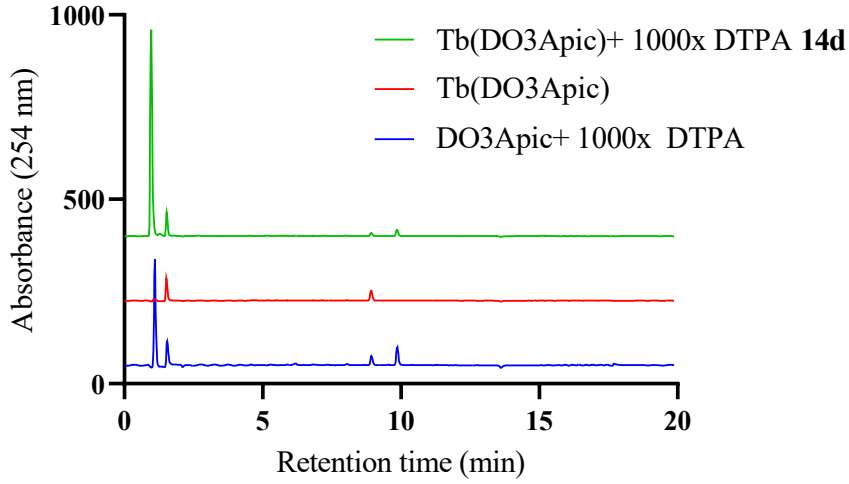

Figure S57. Stability of $[Tb(DO3Apic)]^-$ in the presence of a competing ligand at pH 7.4. HPLC chromatograms were acquired at various time points over a two-week time period. (Method C)

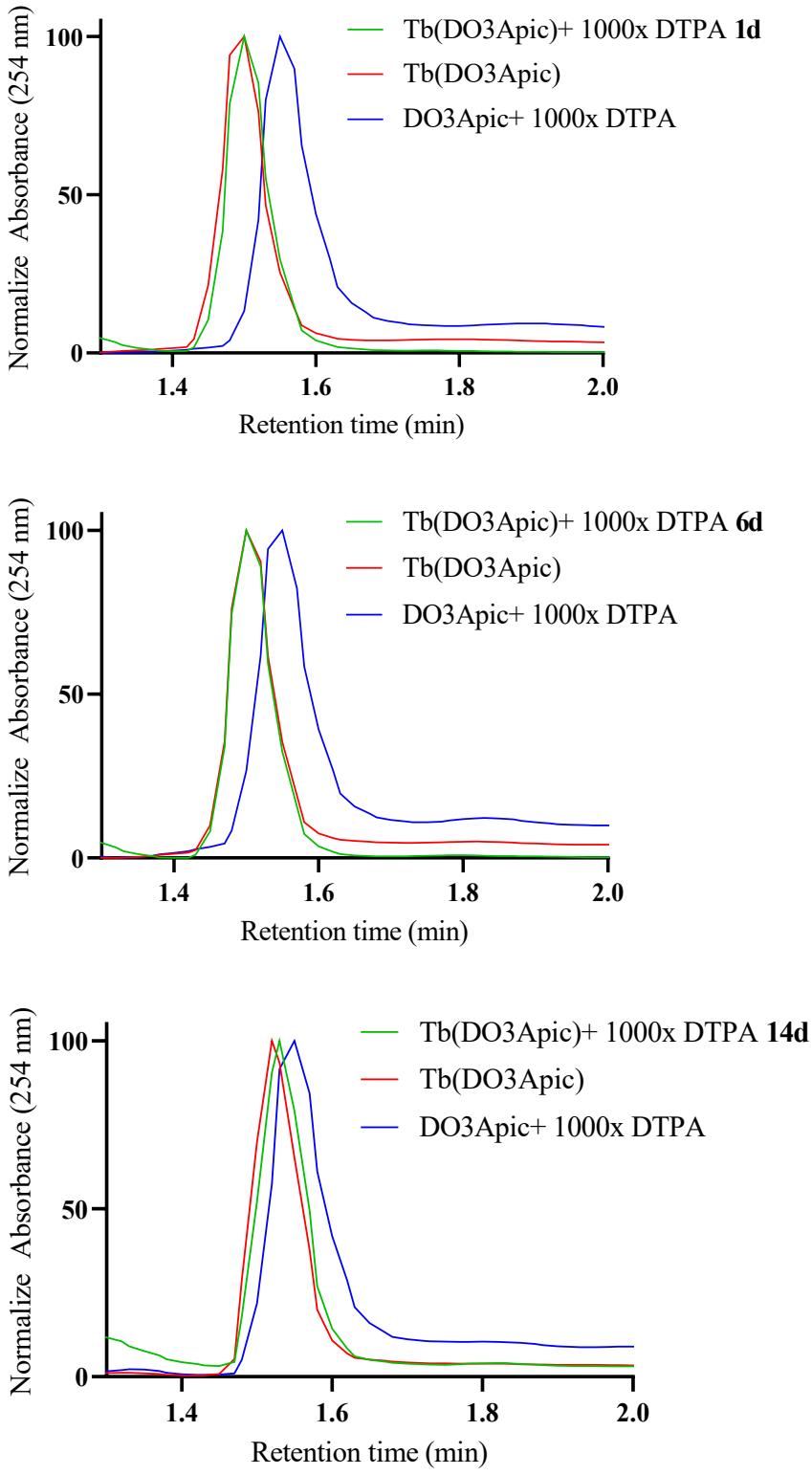

Figure S58. Stability of $[Tb(DO3Apic)]^-$ in the presence of a competing ligand at pH 7.4. HPLC chromatograms were acquired at various time points over a two-week time period. (Method C)

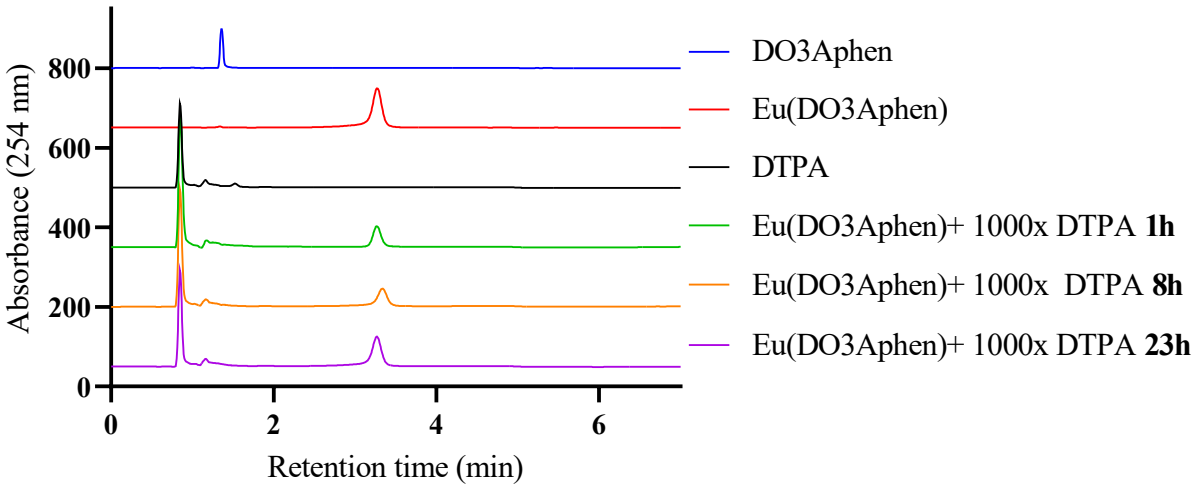

Figure S59. Stability of [Eu(DO3Aphen)] in the presence of a competing ligand at pH 6.5. HPLC chromatograms were acquired at various time points over a 24 hour time period. (Method D)

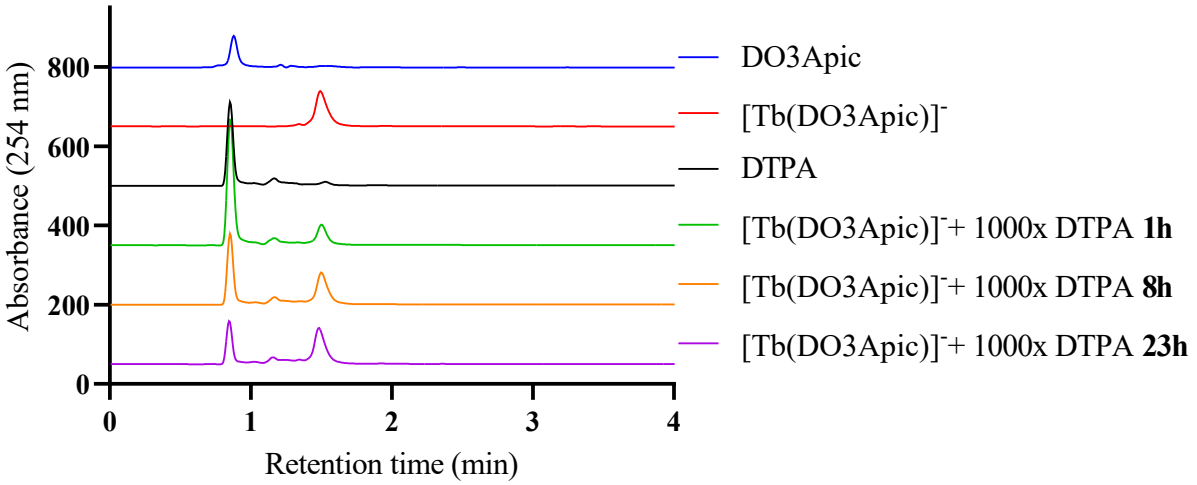

Figure S60. Stability of [Tb(DO3Apic)]$^-$ in the presence of a competing ligand at pH 6.5. HPLC chromatograms were acquired at various time points over a 24 hour time period. (Method D)

3. IVIS Fluorescence Imaging

3.1 Nonfunctionalized Compounds Imaging

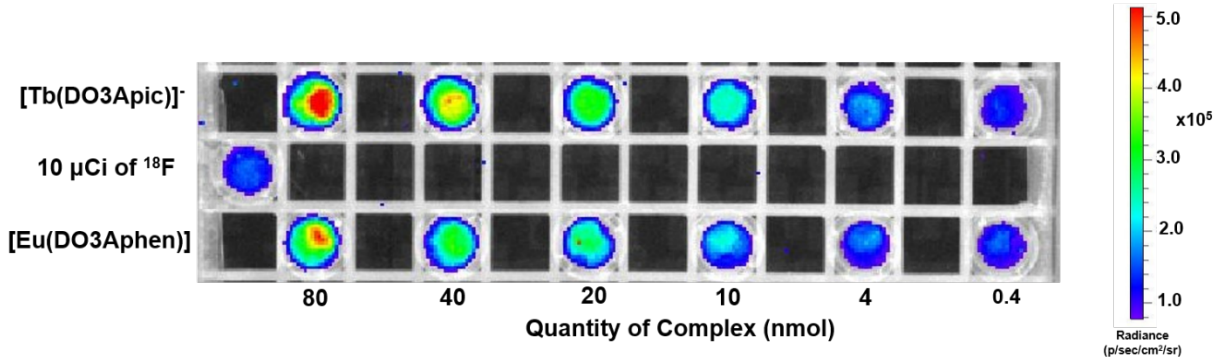

Figure S61. CRET Imaging of [Eu(DO3Aphen)] and $[Tb(DO3Apic)]^-$ in the presence of 10 µCi of $Na^{18}F$

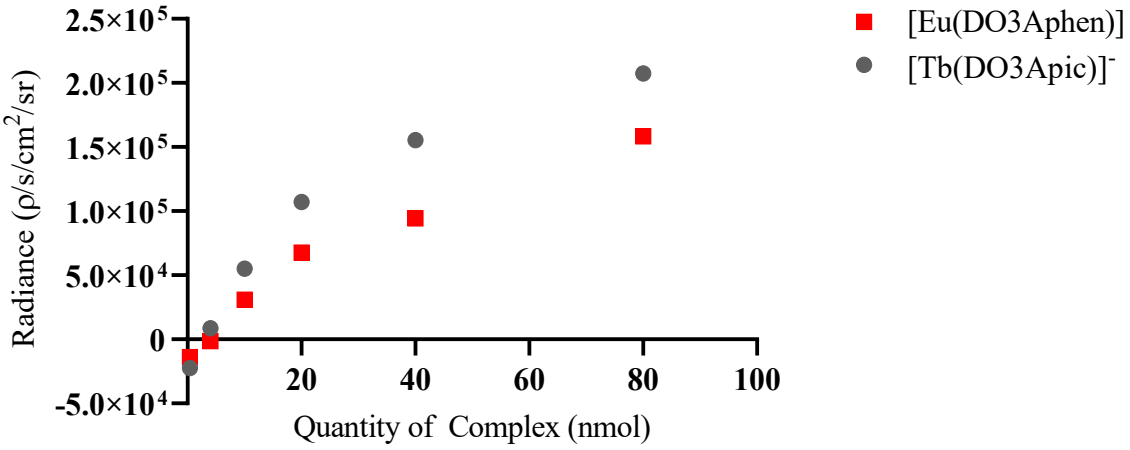

Figure S62. Radiance Quantification, [Eu(DO3Aphen)] and $[Tb(DO3Apic)]^-$ doped with 10 µCi of $Na^{18}F$. n=3. Error bars are shown but are smaller than the data points.

3.2 Effect of Hydration

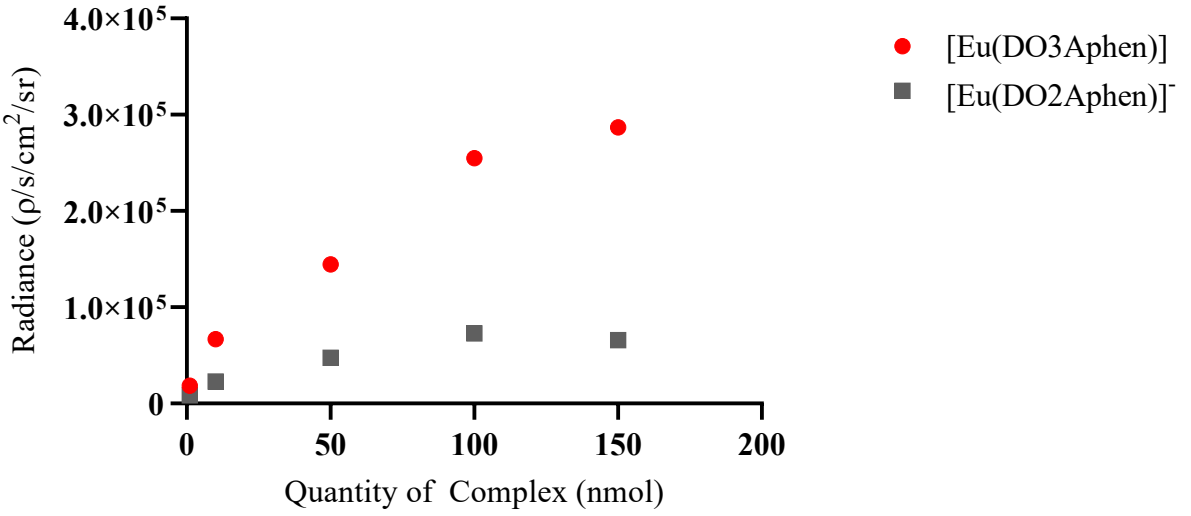

Figure S63. Radiance Quantification, Eu(DO3Aphen) and $[Eu(DO2Aphen)]^+$ doped with 10 µCi of $Na^{18}F$. n=3. Error bars are shown but are smaller than the data points.

3.3 Functionalized Compound Imaging

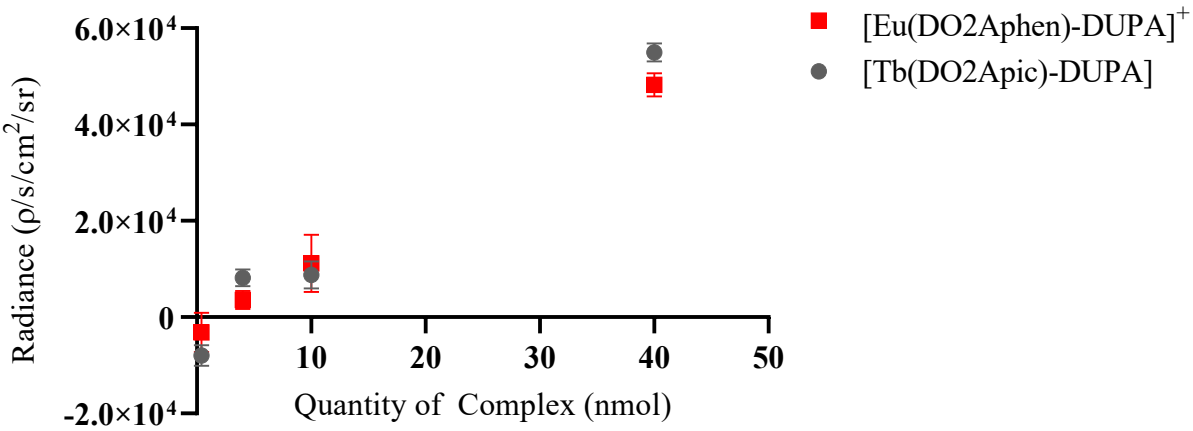

Figure S64. Radiance Quantification, $[Eu(DO2Aphen)\text{-}DUPA]^+$ and [Tb(DO2Apic-DUPA)] doped with 10 µCi of $Na^{18}F$. n=3

3.4 Multiplexed Imaging

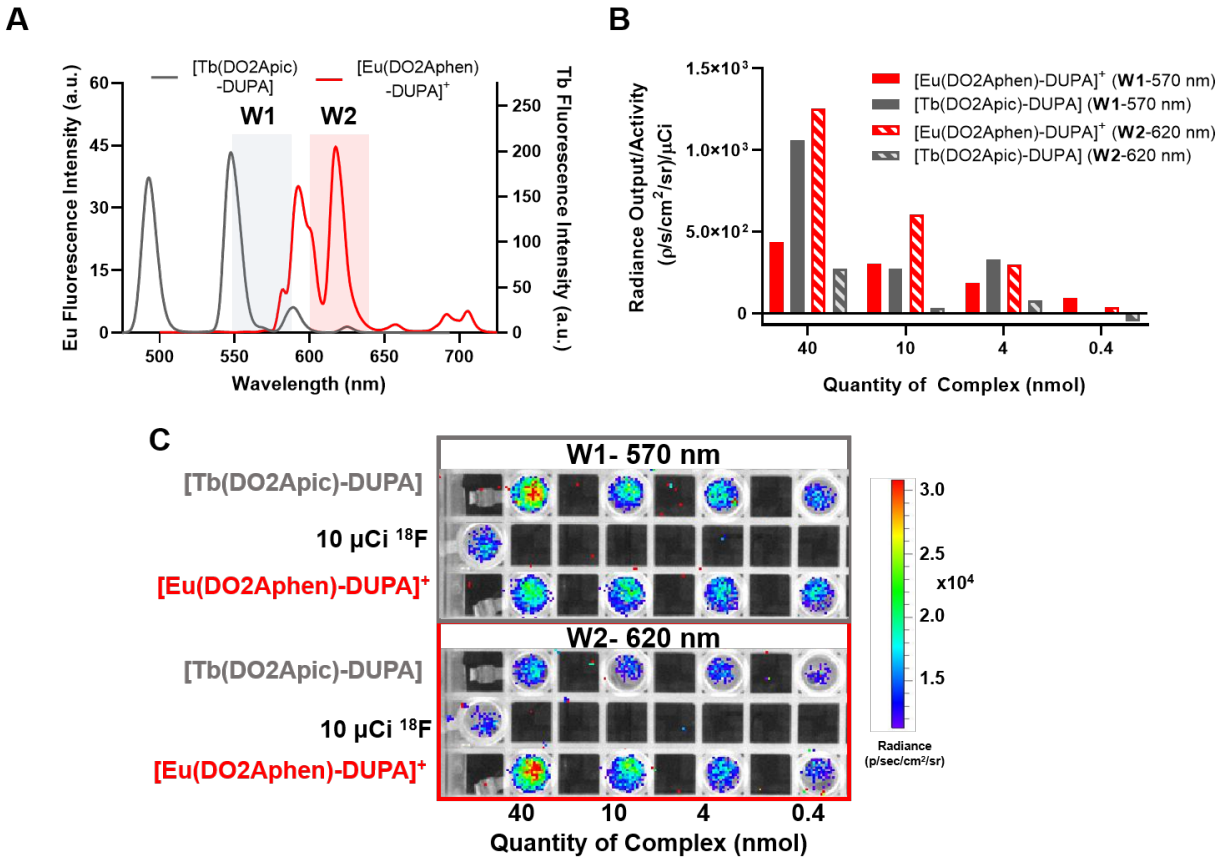

Figure S65. Multiplexed imaging of functionalized complexes. A) Filter windows measured overlaid with the emission spectra of [Eu(DO2Aphen)-DUPA]$^{+}$ and [Tb(DO2Apic)-DUPA]. B) Quantified radiance of the complexes in the presence of 10 µCi of $Na^{18}F$ using region of interest analysis. C) Phantom images of the nonfunctionalized complexes with emission filters of 570 nm and 620 nm in the presence of 10 µCi of $Na^{18}F$.

3.5 Tissue Penetration Imaging

To assess the quenching effects of tissue, phantom images of [Eu(DO2Aphen)-DUPA]$^{+}$ and [Tb(DO2Apic)-DUPA] were collected in the presence of tissue slices (turkey breast). Solutions of 10 and 40 nmol [Eu(DO2Aphen)-DUPA]$^{+}$ and [Tb(DO2Apic)-DUPA] in DPBS were doped with 20 µCi of $Na^{18}F$ and imaged. Turkey slices (2 mm thickness) were layered on top of the phantoms and the samples were reimaged and analyzed as described above.

3.6 In Vivo Imaging

All animal experiments and procedures were performed in accordance with the National Institutes of Health's "Guide for the Care and Use of Laboratory Animals" and approved by Institutional Animal Care and Use Committee (IACUC) at Stony Brook Medicine. Male Ncr mice (Taconic Biosciences, Rensselaer, NY) were inoculated subcutaneously on the right and left shoulders with 1.0 x 10^6 PSMA positive PC-3 PIP cells suspended in Matrigel (1:2 DPBS: Matrigel). When the tumors reached a suitable size, mice were anesthetized with isoflurane and a mixture of [Eu(DO2Aphen)-DUPA]$^+$ (37 nmol) and [^{18}F]-FDG (100 or 22 μCi, NCM-USA, The Bronx, NY) was injected intratumorally to the right shoulder. A corresponding volume of saline and activity of [^{18}F]-FDG (100 or 22 μCi) were injected intratumorally to the left shoulder. Mice were imaged at 5 min (100μCi) and 8 min (22 μCi) p.i. with the IVIS Lumina Series III small animal imager. Mice were sacrificed 3h p.i. (100 μCi dose) and 1h p.i. (22 μCi dose) and tumors were extracted and imaged. Tumors were digested with concentrated nitric acid, diluted and remaining Eu content was determined by ICP-OES. Images were analyzed as described above.

3.7 Quantified Radiance Values

All data has been subtracted from the average radiance value for the Cherenkov only sample.

Table S2. Average Radiance Values, Eu(DO3Aphen) and [Tb(DO3Apic)]$^-$ doped with 10 μCi of Na^{18}F, **open emission**. n=3

Complex	Quantity (nmol)	Average Radiance (ρ/s/cm²/sr)	Standard Deviation
[Eu(DO3Aphen)]	80	158300	4151
	40	94333	1966
	20	67633	1301
	10	30900	1803
	4	-1433	2747
	0.4	-13897	1604
[Tb(DO3Apic)]$^-$	80	207100	5112

	40	155200	5122
	20	107000	4451
	10	55000	1054
	4	8700	1000
	0.4	-22280	1044

Table S3. Average Radiance Values, Eu(DO3Aphen) and $[Tb(DO3Apic)]^-$ doped with 8 μCi of $Na^{18}F$, **windowed to 570 nm**. n=3

Complex	Quantity (nmol)	Average Radiance (ρ/s/cm²/sr)	Standard Deviation
[Eu(DO3Aphen)]	80	9280	852
	40	5773	527
	20	4577	316
	10	2680	1319
	4	-1677	1028
	0.4	-3580	661
$[Tb(DO3Apic)]^-$	80	37450	1057
	40	29737	511
	20	20890	214
	10	12417	182
	4	2633	545
	0.4	-3347	1181

Table S4. Average Radiance Values, Eu(DO3Aphen) and $[Tb(DO3Apic)]^-$ doped with 8 μCi of $Na^{18}F$, **windowed to 620 nm**. n=3

Complex	Quantity (nmol)	Average Radiance (ρ/s/cm²/sr)	Standard Deviation
[Eu(DO3Aphen)]	80	33563	1183
	40	23923	1128
	20	18210	130
	10	11483	337
	4	6060	282
	0.4	1153	75
$[Tb(DO3Apic)]^-$	80	9736	351
	40	7750	85
	20	5036	73
	10	2166	40
	4	-65	81
	0.4	-1439	87

Table S5. Average Radiance Values, Eu(DO3Aphen) and $[Eu(DO2Aphen)]^+$ doped with 10 μCi of $Na^{18}F$. n=3

Complex	Quantity (nmol)	Average Radiance (ρ/s/cm²/sr)	Standard Deviation
[Eu(DO3Aphen)]	150	286967	5590
	100	254700	7238
	50	144600	3928
	10	66700	1664
	1	18533	2060
$[Eu(DO2Aphen)]^-$	150	65700	1510
	100	72700	4732
	50	47633	2822
	10	22800	693
	1	8567	6301

Table S6. Average Radiance Values, $[Eu(DO2Aphen)\text{-}DUPA]^+$ and [Tb(DO2Apic)-DUPA] doped with 10 μCi of $Na^{18}F$, **open emission**. n=3

Complex	Quantity (nmol)	Average Radiance (ρ/s/cm²/sr)	Standard Deviation
$[Eu(DO2Aphen)\text{-}DUPA]^+$	40	48267	2413
	10	11133	5980
	4	3567	1877
	0.4	-3167	4050
[Tb(DO2Apic)-DUPA]	40	54967	1858
	10	8800	2821
	4	8200	1752
	0.4	-8000	2166

Table S7. Average Radiance Values, $[Eu(DO2Aphen)\text{-}DUPA]^+$ and [Tb(DO2Apic)-DUPA] doped with 10 μCi of $Na^{18}F$, **windowed to 570 nm**. n=3

Complex	Quantity (nmol)	Average Radiance (ρ/s/cm²/sr)	Standard Deviation
$[Eu(DO2Aphen)\text{-}DUPA]^+$	40	4347	119
	10	3033	293
	4	1847	105
	0.4	937	123
[Tb(DO2Apic)-DUPA]	40	10580	95
	10	2713	100
	4	3310	193
	0.4	-97	220

Table S8. Average Radiance Values, $[Eu(DO2Aphen)\text{-}DUPA]^+$ and [Tb(DO2Apic)-DUPA] doped with 10 μCi of $Na^{18}F$, **windowed to 620 nm**. n=3

Complex	Quantity (nmol)	Average Radiance (ρ/s/cm²/sr)	Standard Deviation
$[Eu(DO2Aphen)\text{-}DUPA]^+$	40	12543	130
	10	6040	286
	4	2963	81
	0.4	360	115
[Tb(DO2Apic)-DUPA]	40	2753	29
	10	320	125
	4	773	92
	0.4	-493	106

Table S9. Average Radiance Values, $[Eu(DO2Aphen)\text{-}DUPA]^+$ and [Tb(DO2Apic)-DUPA] doped with 20 μCi of $Na^{18}F$, **open emission, no tissue**. n=3

Complex	Quantity (nmol)	Average Radiance (ρ/s/cm²/sr)	Standard Deviation
$[Eu(DO2Aphen)\text{-}DUPA]^+$	40	110433	2450
	10	83367	6407
[Tb(DO2Apic)-DUPA]	40	122700	3516
	10	-9167	6621

Table S10. Average Radiance Values, $[Eu(DO2Aphen)\text{-}DUPA]^+$ and [Tb(DO2Apic)-DUPA] doped with 20 μCi of $Na^{18}F$, **open emission, tissue present**. n=3

Complex	Quantity (nmol)	Average Radiance (ρ/s/cm²/sr)	Standard Deviation
$[Eu(DO2Aphen)\text{-}DUPA]^+$	40	13790	323
	10	6517	710
[Tb(DO2Apic)-DUPA]	40	-1273	745
	10	-5110	704

Table S11. Average Radiance Values, tumors after intertumoral injection of 37 nmol of [Eu(DO2Aphen)-DUPA]$^{+}$ or saline and [^{18}F]-FDG. n=3

Complex	Quantity ^{18}FDG (μCi)	Average Radiance (ρ/s/cm²/sr)	Standard Deviation
[Eu(DO2Aphen)-DUPA]$^{+}$	100	393433	10832
Saline	100	151100	8750
[Eu(DO2Aphen)-DUPA]$^{+}$	22	68383	6348
Saline	22	42687	3046

Table S12. Average Radiance Values, Ex vivo imaging of tumors after intertumoral injection of 37 nmol of [Eu(DO2Aphen)-DUPA]$^{+}$ or saline and [^{18}F]-FDG. n=3

Complex	Quantity ^{18}FDG (μCi)	Average Radiance (ρ/s/cm²/sr)	Standard Deviation
[Eu(DO2Aphen)-DUPA]$^{+}$	100	15829	889
Saline	100	33632	2575
[Eu(DO2Aphen)-DUPA]$^{+}$	22	7440	1213
Saline	22	26566	1785

4. References

1. Cosby, A. G.; Ahn, S. H.; Boros, E., Cherenkov Radiation-Mediated In Situ Excitation of Discrete Luminescent Lanthanide Complexes. *Angew. Chem. Int. Ed.* **2018,** *57* (47), 15496-15499.
2. Kikuchi, K.; Sugihara, F.; Mizukami, S.; Yoshioka, Y.; Matsushita, H.; Nakamura, T., Activatable 19 F MRI Nanoparticle Probes for the Detection of Reducing Environments. *Angew. Chem. Int. Ed.* **2014,** *54* (3), 1007-1010.
3. Lim, N.-H.; Ding-Pfennigdorff, D.; Nagase, H.; Hu, H.-Y.; Wendt, K. U.; Schultz, C.; Plettenburg, O.; Saas, J.; Nazare, M.; Ritzeler, O., DOTAM Derivatives as Active Cartilage-Targeting Drug Carriers for the Treatment of Osteoarthritis. *Bioconjugate Chem.* **2015,** *26* (3), 383-388.
4. Kularatne, S. A.; Zhou, Z.; Yang, J.; Post, C. B.; Low, P. S., Design, Synthesis, and Preclinical Evaluation of Prostate-Specific Membrane Antigen Targeted 99m Tc-Radioimaging Agents. *Mol. Pharmaceutics* **2009,** *6* (3), 790-800.
5. Aluicio-Sarduy, E.; Thiele, N. A.; Martin, K. E.; Vaughn, B. A.; Devaraj, J.; Olson, A. P.; Barnhart, T. E.; Wilson, J. J.; Boros, E.; Engle, J. W., Establishing Radiolanthanum Chemistry for Targeted Nuclear Medicine Applications. *Chem. Eur. J.* **2020,** *26* (6), 1238-1242.
6. Quici, S.; Gianolio, E.; Anelli, P. L.; Accorsi, G.; Botta, M.; Marzanni, G.; Armaroli, N.; Cavazzini, M.; Barigelletti, F., Highly Luminescent Eu 3+ and Tb 3+ Macrocyclic Complexes Bearing an Appended Phenanthroline Chromophore. *Inorg. Chem.* **2002,** *41* (10), 2777-2784.
7. Beeby, A.; Parker, D.; de Sousa, A. S.; Clarkson, I. M.; Woods, M.; Faulkner, S.; Dickins, R. S.; Royle, L.; Williams, J. A. G., Non-radiative deactivation of the excited states of europium, terbium and ytterbium complexes by proximate energy-matched OH, NH and CH oscillators: an improved luminescence method for establishing solution hydration states. *J. Chem. Soc., Perkin Trans. 2* **1999,** *2* (3), 493-504.